A journey in the world of

Blue spinels

Nicolas HÉBERT

43rd Australasian mineralogical societies conference

4th October 2020


Specimen from N.Gilly 38*25*14 mm
Ali Abad, Hunza Valley, Hunza District, Gilgit-Baltistan, Pakistan

50 shades of blue spinel

“Jay” Sri-Lankan spinel

8.70 ct, coll GEMATRIX
Photography : Alexey Jurys Yakhlakov

https://gem-matrix.com/collection/single/tproduct/202544733-502365255783-jay-spinel-870-cts

Blue Spinel 12.42 cts

$16 394

Jay Spinel 2.80 cts

$2 800

Jay Spinel 3.99 cts

$4 700

Jay Spinel 2.99 cts

$2 300

Jay Spinel 3.33 cts

$2 160

Jay Spinel 4.34 cts

$4 000

https://gem-matrix.com/collection/single?s_recid=202544733&s_charact%3A351638=Greyish-Blue#spinel

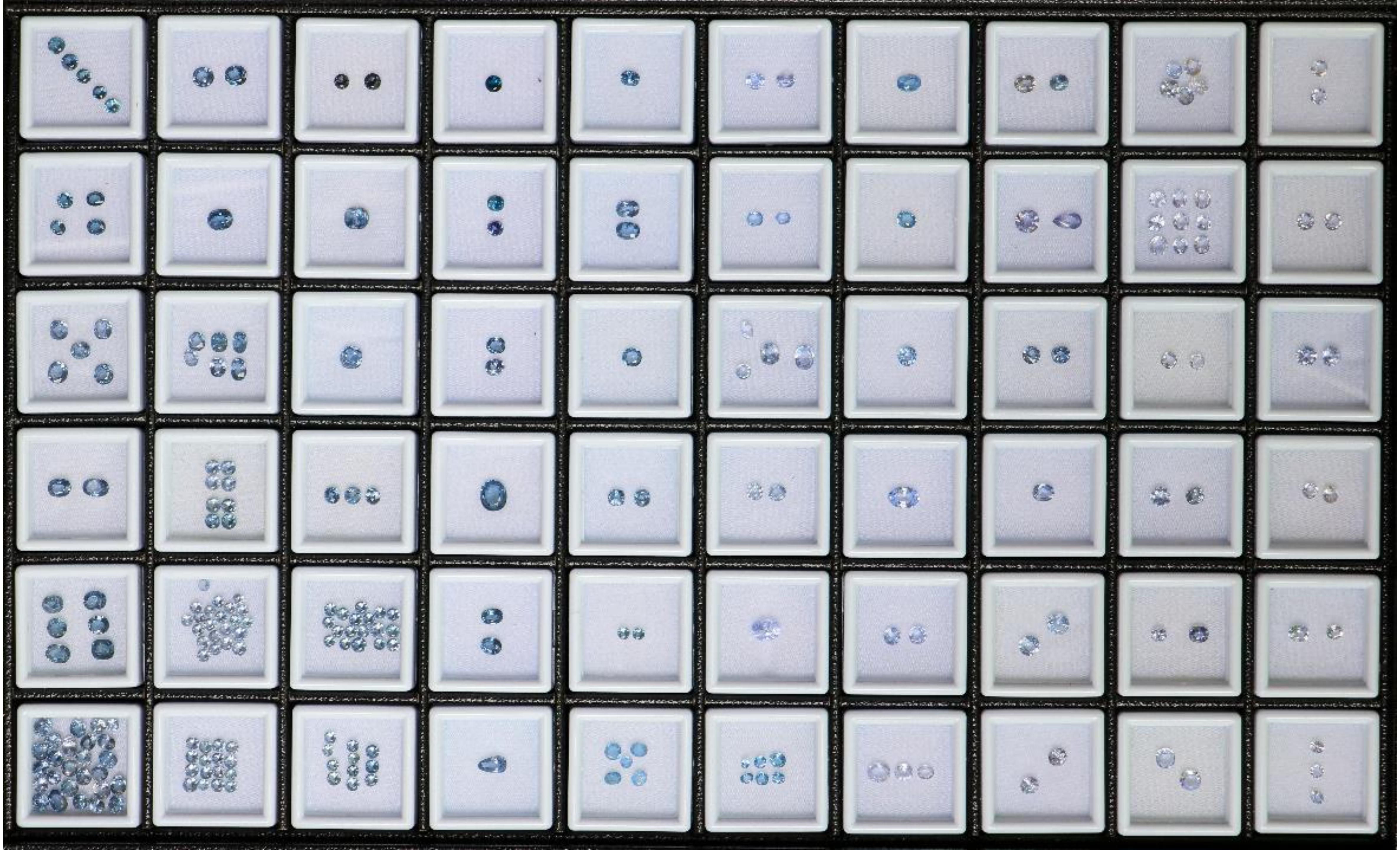

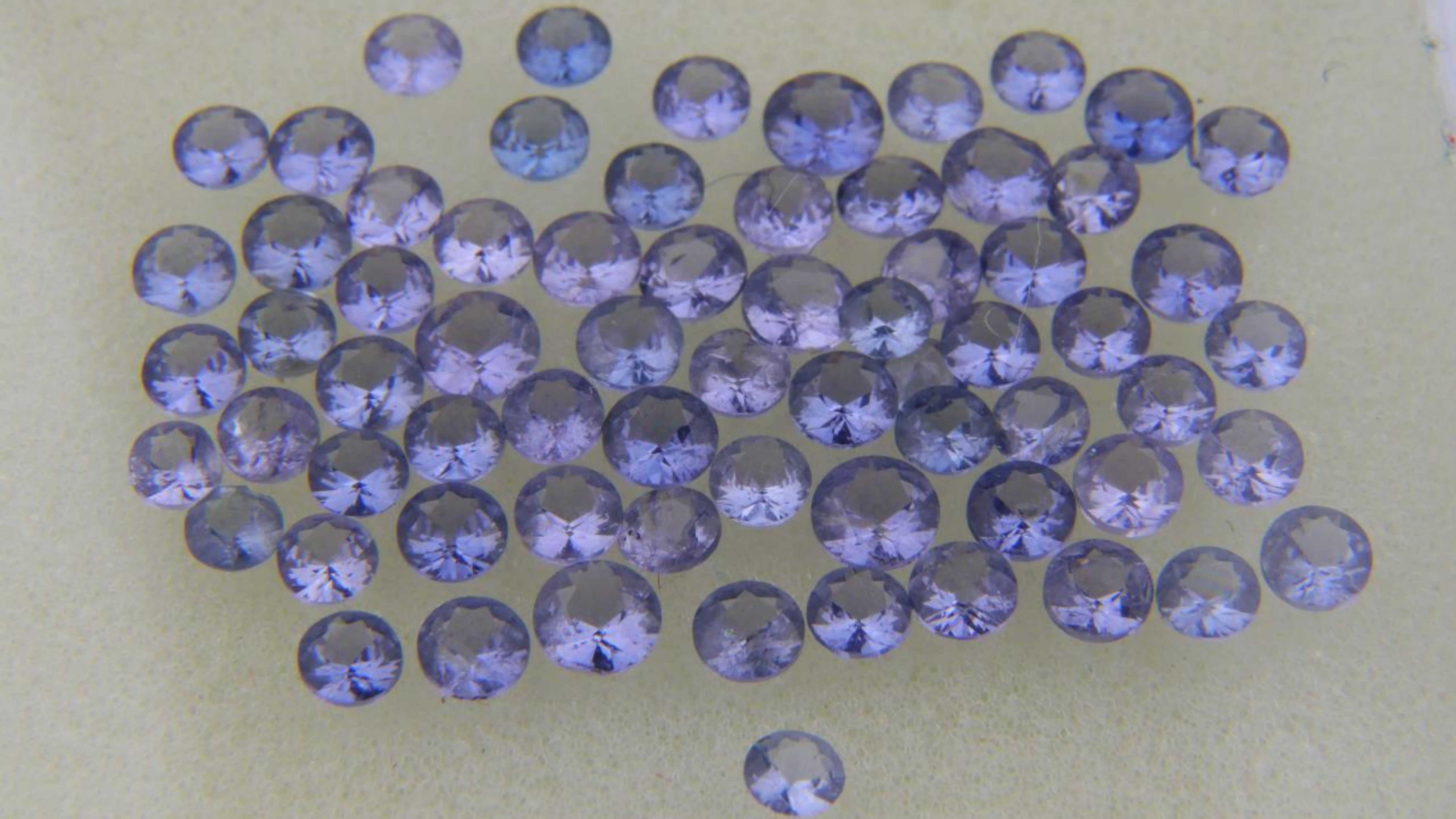

Lavender Spinel Burma
8.51 cts

Lavender Spinel Burma
6.93 cts

Grey Spinel 10.90 cts / 2 pcs
$7,412.00

Spinel 4.73 cts / 2 pcs
$426.00

Lavender Spinel 4.57 cts

Lavender Spinel 7.03 cts

Violet Spinel 7.48 cts

Lavender Spinel 11.78 cts / 2 pcs

Luc Yen spinels

private collection of Min Tran

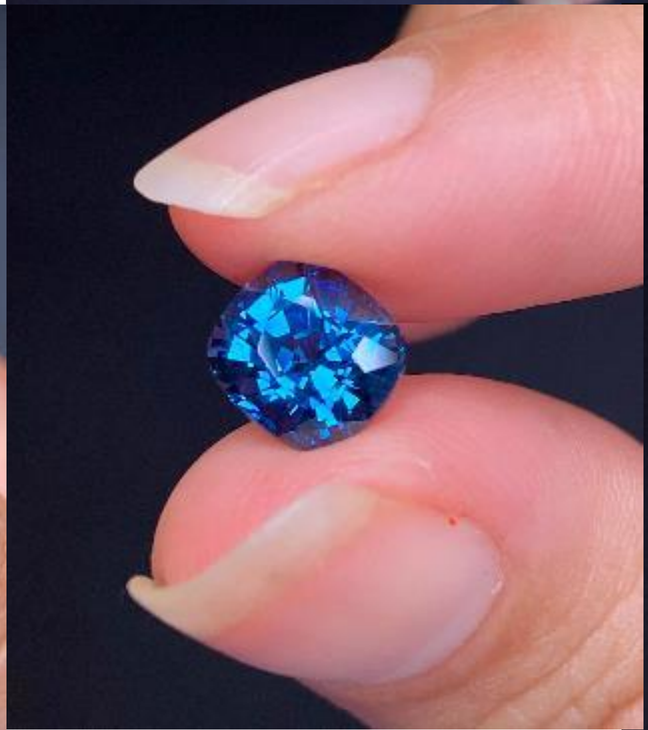

Cobalt Neon Blue Spinel 0.23 ct
$1,800.00

Cobalt Neon Blue Spinel 0.26 ct
$1,800.00

Cobalt Neon Blue Spinel 0.21 ct
$990.00

Cobalt Neon Blue Spinel 0.22 ct
$680.00

Cobalt Blue Spinel 0.29 ct
$590.00

Cobalt Neon Blue Spinel 0.25 ct
$490.00

Cobalt Neon Blue Spinel 0.22 ct
$460.00

Cobalt Neon Blue Spinel 0.06 ct
$460.00

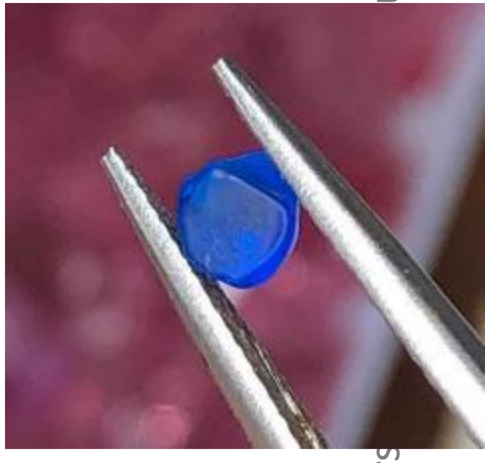

Photo and specimen, Gem Atle Gussias, BalderGems

https://yavors ue-s

Spinel : a simple formula

- $MgAl_2O_4$

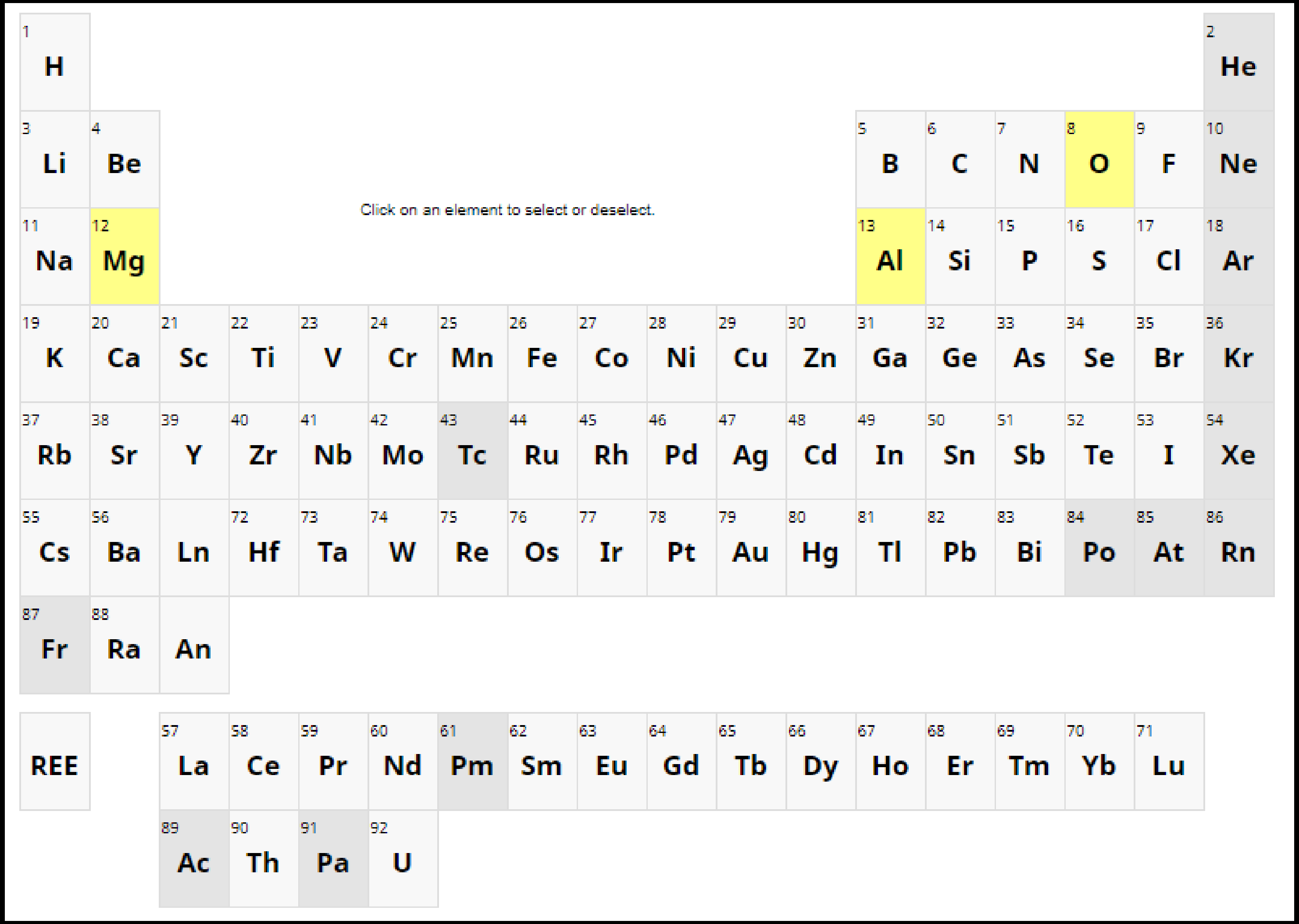

Spinel : a simple formula ?

- $A^{2+}B^{3+}{}_2X_4$

- $Fe^{2+}\,Al^{3+}{}_2O_4$ Hercynite
- $Fe^{2+}\,Fe^{3+}{}_2O_4$ Magnetite
- $Zn^{2+}Al^{3+}{}_2O_4$ Gahnite
- $Fe^{2+}Cr^{3+}{}_2O_4$ Chromite
- $Mg^{2+}Cr^{3+}{}_2O_4$
  Magnesiochromite

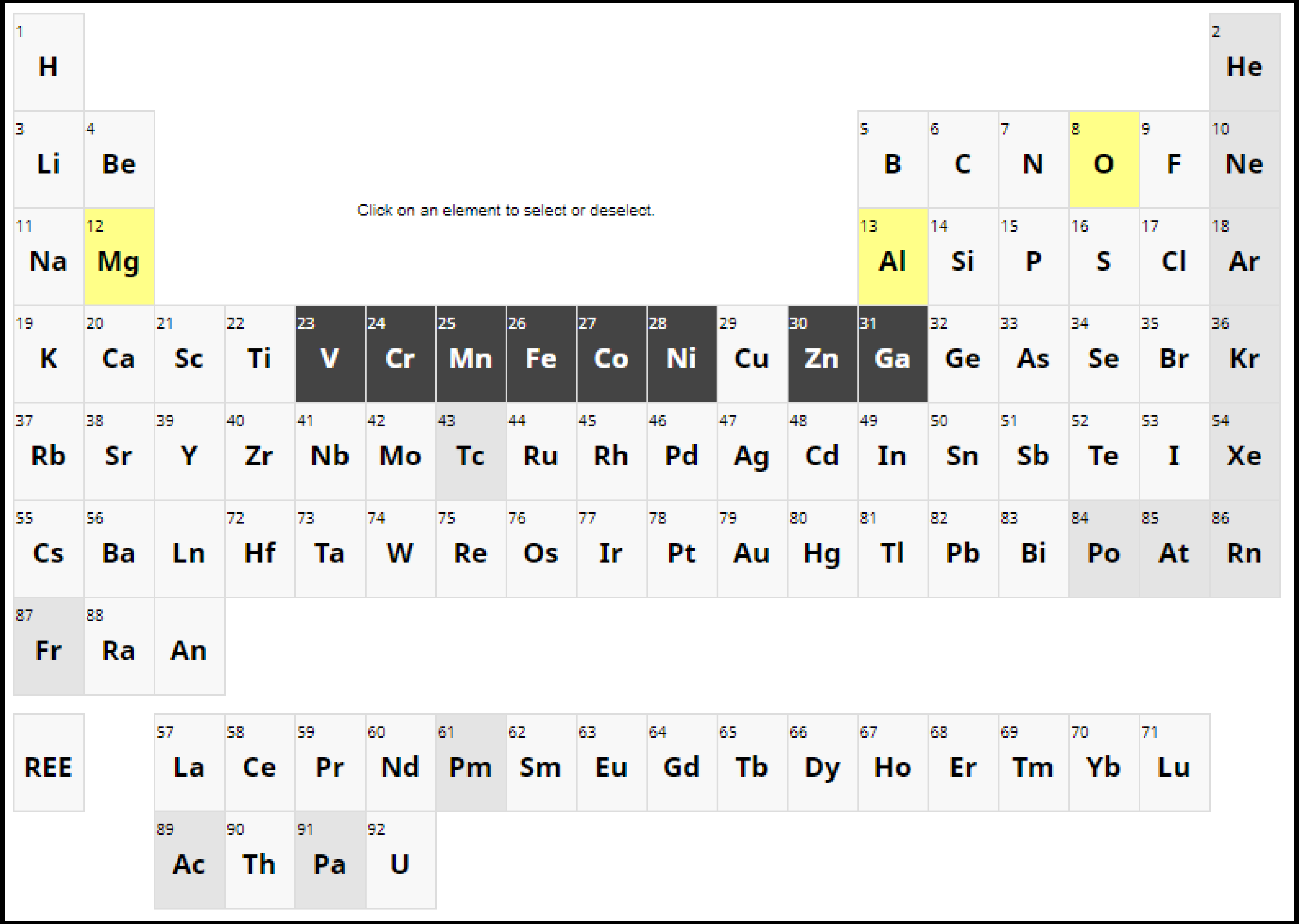

Spinel : a not so simple formula

- $A^{2+}B^{3+}{}_2X_4$
- (Mg,Fe,Zn,Co,Mn,Ni) $^{2+}$ (Al,Fe,Cr,V) $^{3+}{}_2$ O_4

Spinel : colors of the rainbow

- $A^{2+}B^{3+}{}_2X_4$
- $(Mg,Fe,Zn,Co,Mn,Ni)^{2+}(Al,Fe,Cr,V)^{3+}{}_2O_4$

BOX A: FLUX SYNTHETIC SPINELS OF OTHER COLORS

Besides the red and blue samples described in this article, Russian laboratories have grown other colors of flux synthetic spinel, apparently on an experimental basis (W. Barshai, pers. comm., 1991). We studied three brownish yellow octahedra or octahedral fragments ranging from 0.29 to 3.76 ct, one 3.34-ct greenish blue crystal, one 0.80-ct purple elongated octahedron, and one 1.43-ct pale pink crystal (figure A-1). Their indices of refraction and specific-gravity values were within the ranges measured for red and blue natural and flux synthetic spinels, as described in the article text (except for the pink crystal, which had a low S.G., 3.55). These other colors all showed slight anomalous birefringence ("strain"); three exhibited "snake-like bands" under crossed polarizers. All but the inclusion-free purple and pale pink stones displayed typical orange-brown flux inclusions.

The three brownish yellow spinels fluoresced a weak to moderate chalky yellowish green to long-

Figure A-1. Russian laboratories have produced flux-grown synthetic spinels in a variety of colors other than red and blue. These samples, reportedly grown on an experimental basis, range from 0.80 to 3.76 ct. Photo by Maha DeMaggio.

Muhlmeister et al, Gems and gemology 2013,81-98

Structural mineralogy

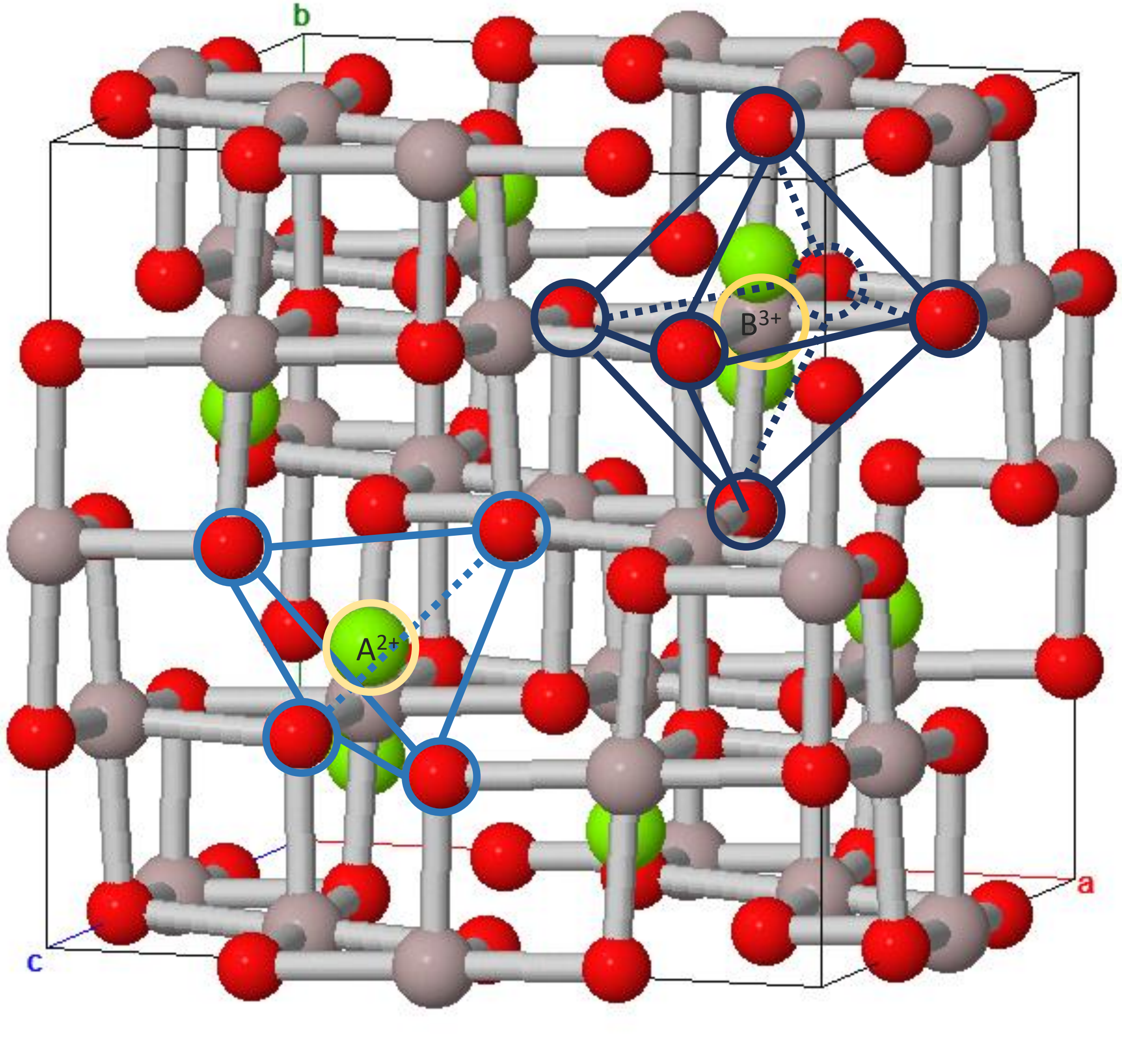

Octahedral site (M) for trivalent cations

Tetrahedral site (T) for divalent cations

Laws are meant to be brocken

Andreozzi et al, *Phys Chem Minerals* **46,** 343–360 (2019).
https://doi.org/10.1007/s00269-018-1007-5
Le Thi Thu Huong, Vietnam Journal of Earth Sciences, 40(1), 47-55, Doi:10.15625/0866-7187/40/1/10915

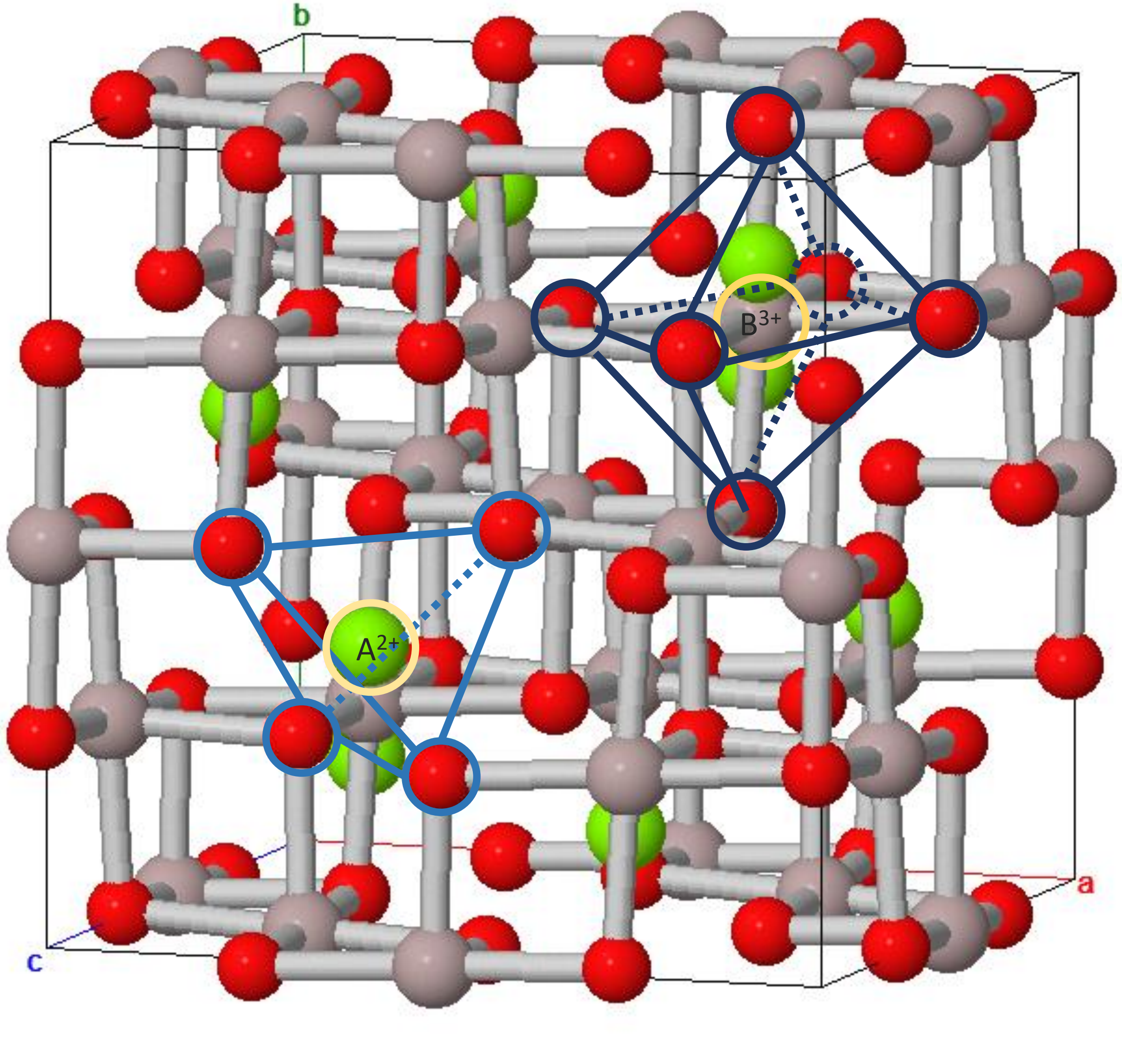

Octahedral site (M) for trivalent cations

$(Al,Fe,Cr,V)^{3+}$

Tetrahedral site (T) for divalent cations

$(Mg,Fe,Zn,Co,Mn,Ni)^{2+}$

A world of possible substitutions

- The color of samples with a pink (incl. lilac and pale violet), blue and green hue is essentially influenced by the Fe content, and specifically by Fe^{2+}/Fe^{3+} ratios, even if a clear attribution is not straightforward.
- 670275 $T(Mg_{0.838}Al_{0.083}Fe^{2+}_{0.056}Fe^{3+}_{0.006}Zn_{0.006}Mn_{0.004})\Sigma_{0.993}M(Al_{1.870}Mg_{0.104}Fe^{2+}_{0.002}Ti_{0.001})\Sigma_{1.995}O_4$
- 881728 $T(Zn_{0.839}Fe^{2+}_{0.080}Mg_{0.056}Al_{0.024}Mn_{0.001})\Sigma_{1.000}M(Al_{1.914}Fe^{3+}_{0.026}Fe^{2+}_{0.024}V^{3+}_{0.001})\Sigma_{1.999}O_4$

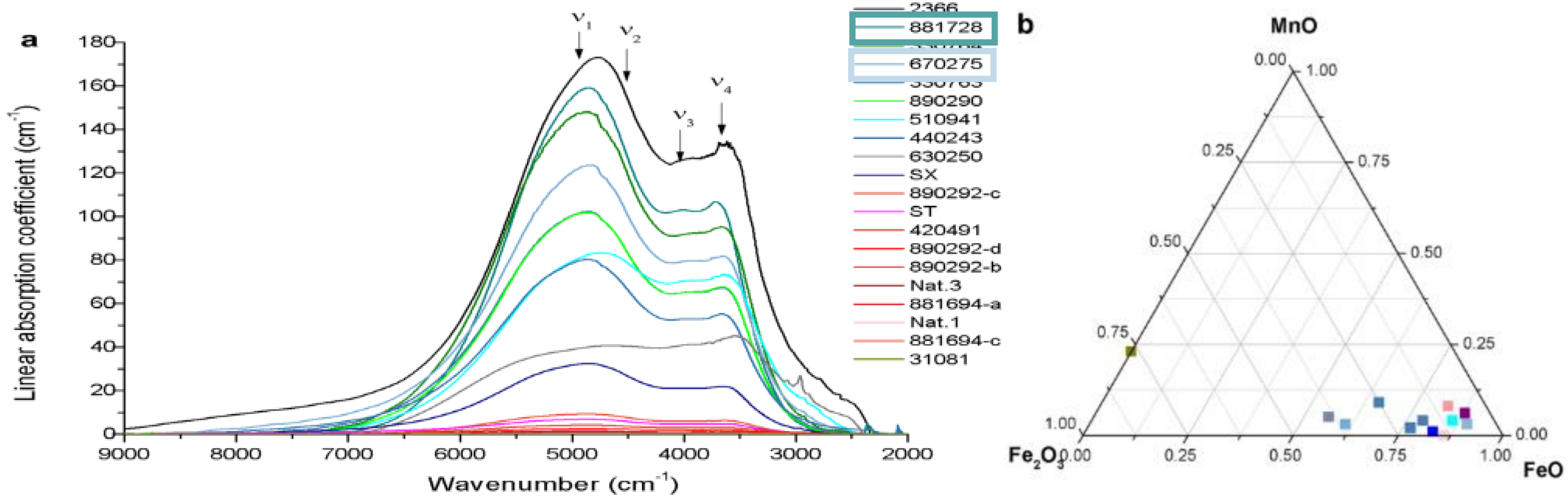

Andreozzi et al, *Phys Chem Minerals* **46,** 343–360 (2019). https://doi.org/10.1007/s00269-018-1007-5

Signal decomposition

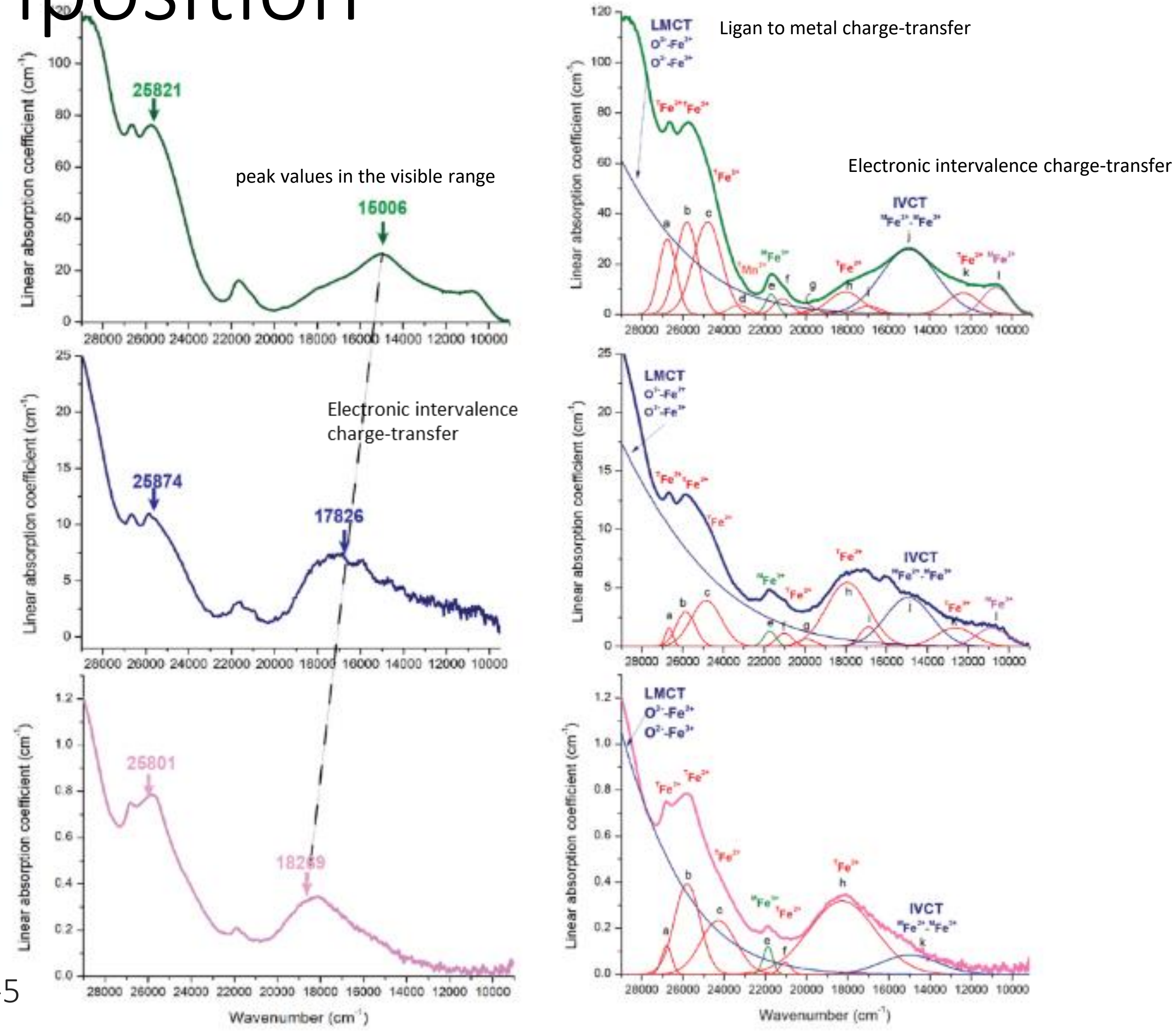

Andreozzi et al, *Phys Chem Minerals* **46,** 343–360 (2019). https://doi.org/10.1007/s00269-018-1007-5


Spinel-Hercynite solid solution
^{M}Fe
^{M}Fe
^{M}Fe
Blue light increased absorption due to the 14,500 cm^{-1} band related to $^{M}Fe^{2+}$ - $^{M}Fe^{3+}$ InterValence Charge Transfert (Non-linear)

6 shades of blue spinel, illustrated

Label	Nat.2	Nat.4	30070	440243	510942	800801
						
Color	Light blue	Greenish blue	Dark blue	Purplish blue	Blue	Blue
Origin	Tunduru, Tanzania	Tunduru, Tanzania	New Jersey, USA	Åker, Sweden	Levida, Spain	Catanzaro, Italy

Table 4 Chemical formulae of the investigated natural blue spinel samples (in apfu). The dominant component at the respective cation site is written in bold

apfu atoms per formula unit. Fe^{2+} and Fe^{3+} contents from charge balance

Nat. 2	$(\mathbf{Mg}_{0.974}Zn_{0.003}Fe^{2+}_{0.025})_{\Sigma 1.002}(\mathbf{Al}_{1.988}Fe^{3+}_{0.008}Si_{0.002})_{\Sigma 1.998}O_4$
Nat. 4	$(\mathbf{Mg}_{0.985}Zn_{0.001}Fe^{2+}_{0.016})_{\Sigma 1.002}(\mathbf{Al}_{1.984}Fe^{3+}_{0.012}Cr_{0.001}Si_{0.001})_{\Sigma 1.998}O_4$
30070	$(Mg_{0.007}\mathbf{Zn}_{0.981}Fe^{2+}_{0.018})_{\Sigma 1.006}(\mathbf{Al}_{1.964}Fe^{3+}_{0.024}Si_{0.006})_{\Sigma 1.994}O_4$
440243	$(\mathbf{Mg}_{0.952}Zn_{0.010}Fe^{2+}_{0.037}Mn_{0.003})_{\Sigma 1.002}(\mathbf{Al}_{1.983}Fe^{3+}_{0.012}Si_{0.002}Ti_{0.001})_{\Sigma 1.998}O_4$
510942	$(Mg_{0.060}\mathbf{Zn}_{0.797}Fe^{2+}_{0.140}Mn_{0.004})_{\Sigma 1.001}(\mathbf{Al}_{1.984}Fe^{3+}_{0.012}Si_{0.002}V_{0.001})_{\Sigma 1.999}O_4$
800801	$(\mathbf{Mg}_{0.856}Zn_{0.094}Fe^{2+}_{0.045}Mn_{0.007}Co_{0.002})_{\Sigma 1.004}(\mathbf{Al}_{1.979}Fe^{3+}_{0.014}Si_{0.003})_{\Sigma 1.996}O_4$

D'Ippolito, V., Andreozzi, G.B., Hålenius, U. et al. Color mechanisms in spinel: cobalt and iron interplay for the blue color. Phys Chem Minerals 42, 431–439 (2015). https://doi.org/10.1007/s00269-015-0734-0

Gahnite, Kagoro, Kaduna state, Nigeria

- $^{T}(Zn_{0.94}Fe^{2+}_{0.03}Al_{0.03})\ ^{M}(Al_{1.96}\ Fe^{2+}_{0.03}\ Fe^{3+}_{0.01})\ O_4$
- Very small amounts of Mg and Mn^{2+} (<0.005 a.p.f.u.) occur at T sites.

https://joehenleyrough.com/collections/spinel-crystals/products/blue-spinel-crystal

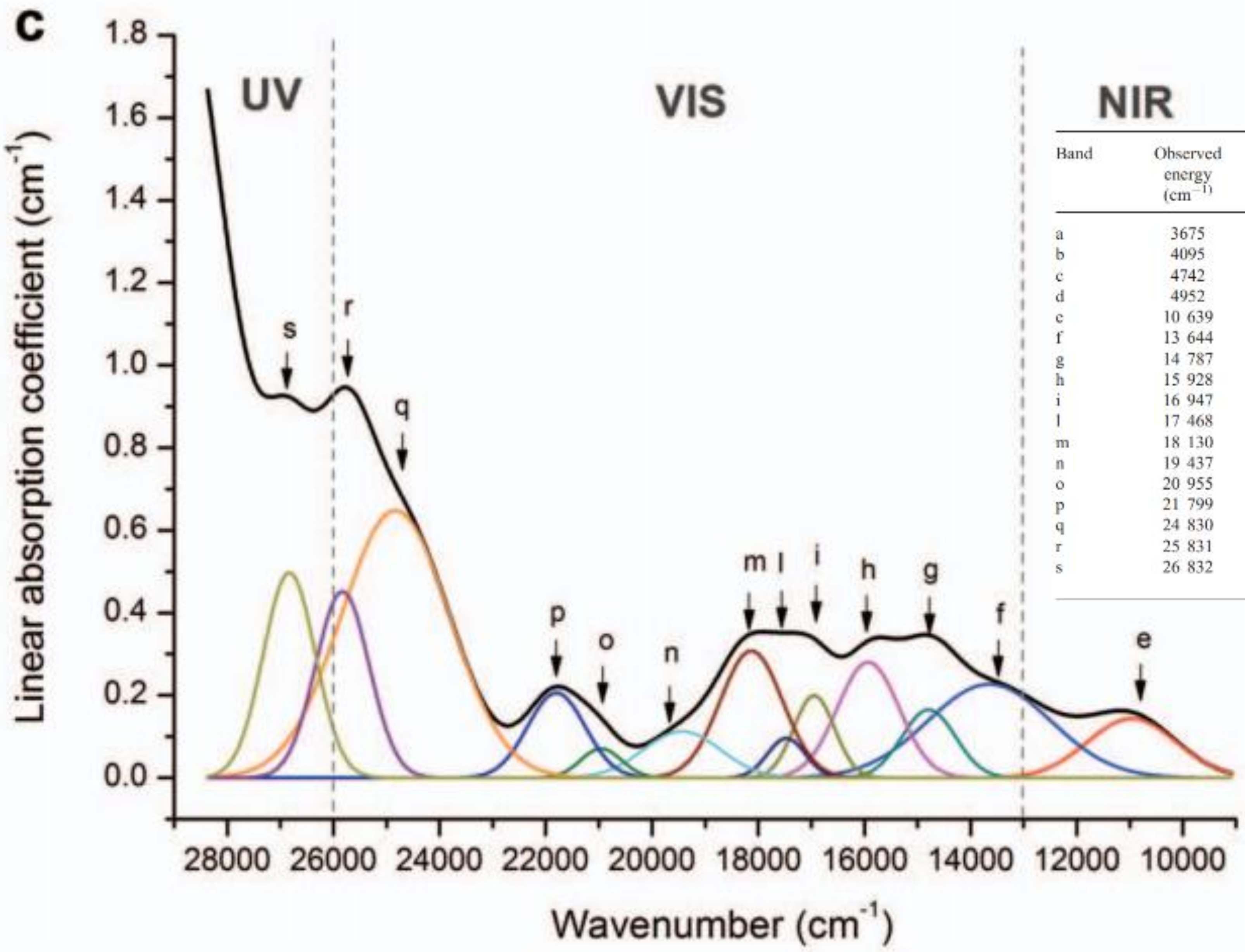

Band	Observed energy (cm^{-1})	Linear absorption coefficient (cm^{-1})	Band width FMHW (cm^{-1})	Assignment
a	3675	79	555	spin allowed *d–d* transitions $^5E \rightarrow {}^5T_2$ in $^TFe^{2+}$ and splitting due to dynamic Jahn-Teller effect
b	4095	25	394	
c	4742	18	630	
d	4952	132	1547	
e	10 639	0.14	1968	spin-allowed *d–d* transition $^5T_{2g} \rightarrow {}^5E_g$ in $^MFe^{2+}$
f	13 644	0.23	2739	spin-forbidden transitions $^5E \rightarrow {}^3T_1$ of $^TFe^{2+}$
g	14 787	0.17	1185	spin-forbidden transitions $^5T_1 \rightarrow {}^5E$ of $^TFe^{2+}$
h	15 928	0.28	1368	$^MFe^{2+} \leftrightarrow {}^MFe^{3+}$ IVCT
i	16 947	0.20	907	spin-forbidden transitions $^5E \rightarrow {}^3E$ of $^TFe^{2+}$
l	17 468	0.10	840	spin-forbidden transitions $^5E \rightarrow {}^3T_1$ of $^TFe^{2+}$
m	18 130	0.31	1385	spin-forbidden transitions $^5E \rightarrow {}^3T_2$ of $^TFe^{2+}$
n	19 437	0.11	1710	spin-forbidden transitions $^5E \rightarrow {}^3A_2$, $^3A_1$ of $^TFe^{2+}$
o	20 955	0.07	905	$^6A_{1g} \rightarrow {}^4A_{1g}$, ^4E_g transition of $^MFe^{3+}$
p	21 799	0.21	1277	spin-forbidden transitions $^5E \rightarrow {}^3T_2$, $^3T_1$, ^3E of $^TFe^{2+}$
q	24 830	0.65	2414	spin-forbidden transitions $^5E \rightarrow {}^3T_2$, $^3T_1$ of $^TFe^{2+}$
r	25 831	0.45	1186	
s	26 832	0.50	1155	spin-forbidden transitions $^5E \rightarrow {}^3E$ of $^TFe^{2+}$

V. D'Ippolito; et al Mineralogical Magazine (2013) 77 (7): 2941–2953.
https://doi.org/10.1180/minmag.2013.077.7.05

To put it simply, a spinel is a mixture of

Tetrahedral [T]

($Mg^{2+}Fe^{2+}Zn^{2+}Mn^{2+}Co^{2+}Ni^{2+}Al^{3+}$)$_{\Sigma 1}$

Octahedral[M]

(Al^{3+} $Fe^{3+}Fe^{2+}$ V^{3+} Cr^{3+} $Ti^{3+}Mg^{2+}$ Co^{2+} Fe^{2+})$_{\Sigma 2}$ O_4

$Fe^{3+}Fe^{2+}$

$Fe^{3+}Fe^{2+}$

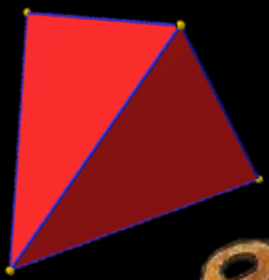

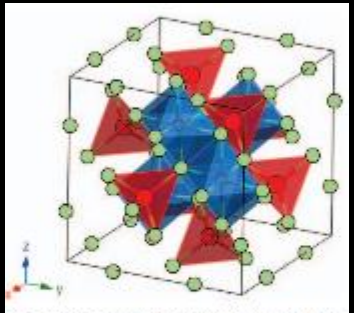

Fig. 1. Spinel structure, with the cubic unit cell outlined in black, oxygen ions in green, tetrahedra and T sites in red and octahedra and M sites in blue.

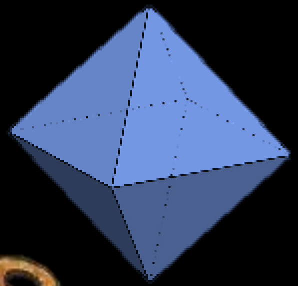

D'IPPOLITO et al, Mineralogical Magazine, October 2013, Vol. 77(7), pp. 2941–2953

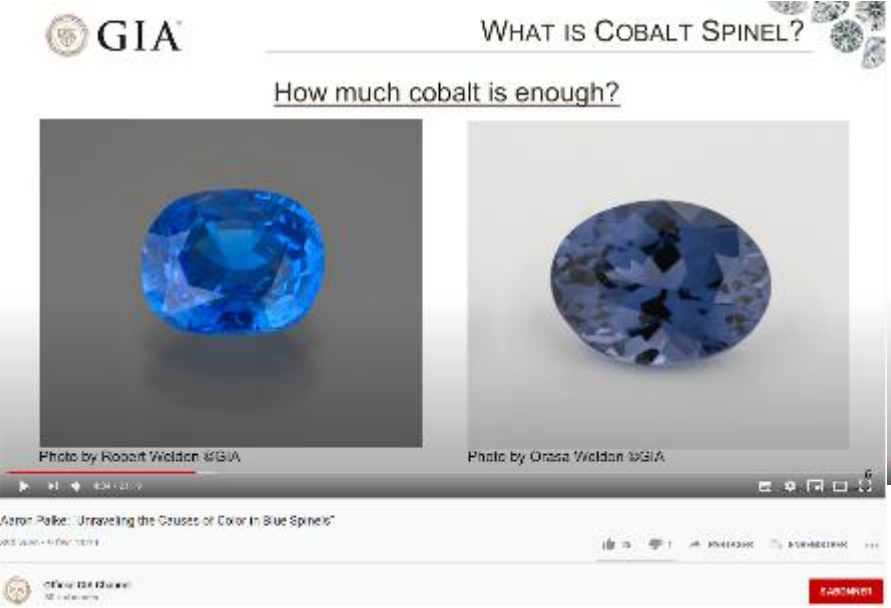

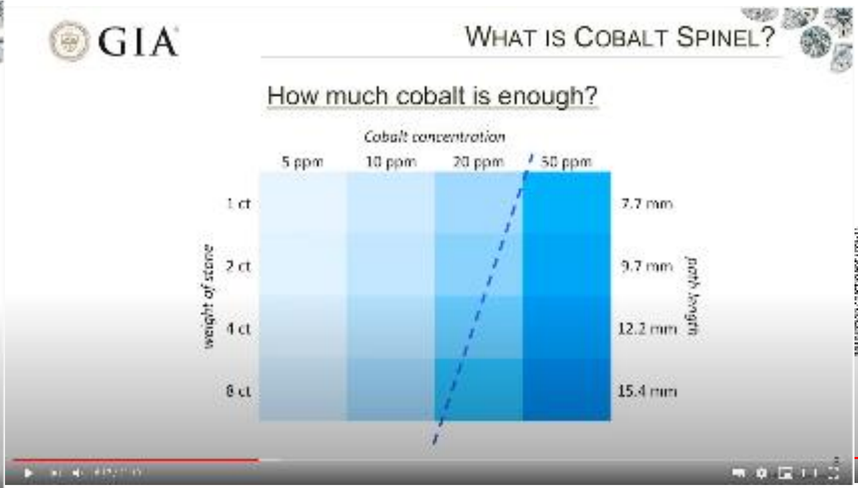

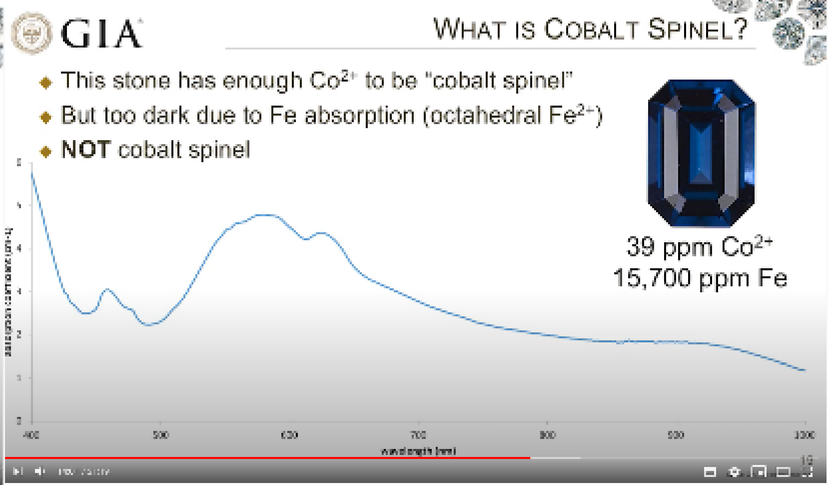

Ultimate definition of cobalt spinel : a sterile debate ?

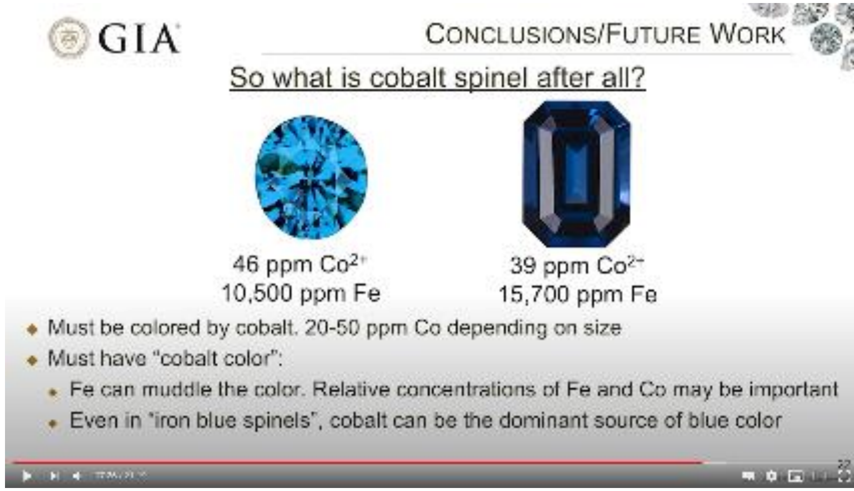

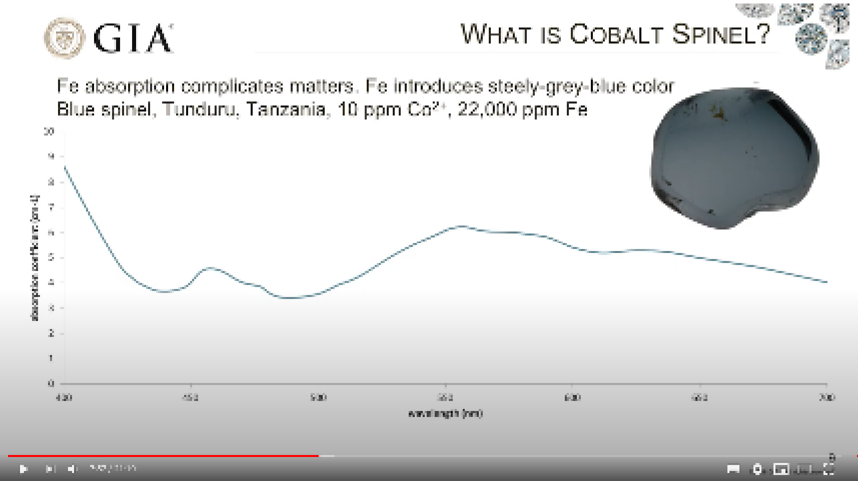

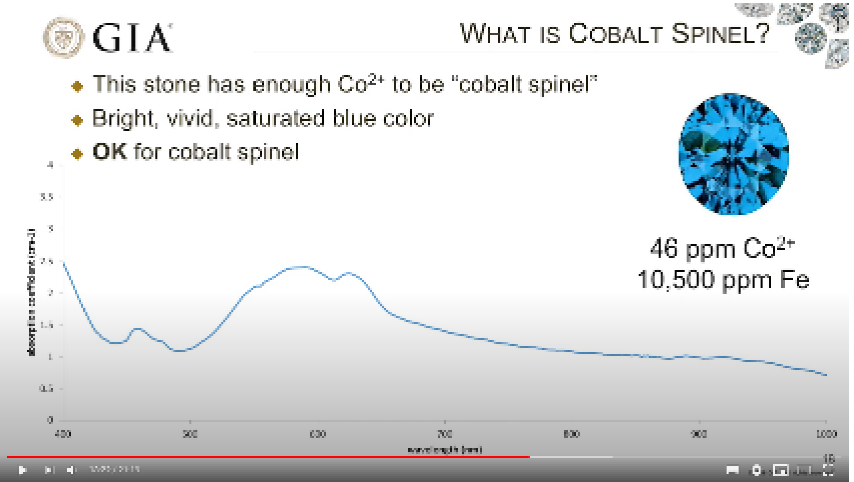

So, Cobalt or not Cobalt ?

This is the question !

icant. The term "cobalt-blue" can be clarified by further investigations on the significance of each chromophore elements (iron and cobalt). These investigations can propose a limit on the ratio of iron/cobalt above which the term "cobalt-blue" cannot be used.


```
IF((Fe/Co) ≪ 10), Cobalt_spinel == TRUE)
```

Wrong , because iron doesn't have a linear behaviour !

$$\frac{250\ ppm\ Fe}{25\ ppm\ Co} \neq \frac{2500\ ppm\ Fe}{250\ ppm\ Co} \neq \frac{10000\ ppm\ Fe}{1000\ ppm\ Co}$$

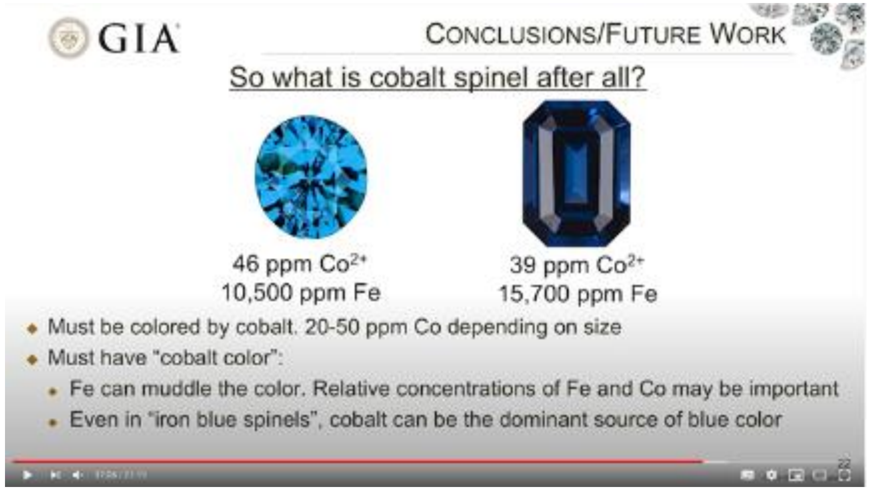

"One cannot mix potatoes and carots but for soup"

A consistent approach to quantify color

- The CIE colorimetric coordinates, lightness
  - L* (black–white),
  - a* (green–red)
  - b* (blue–yellow)

Are measured using a Konica-Minolta Chroma Meter CR-400

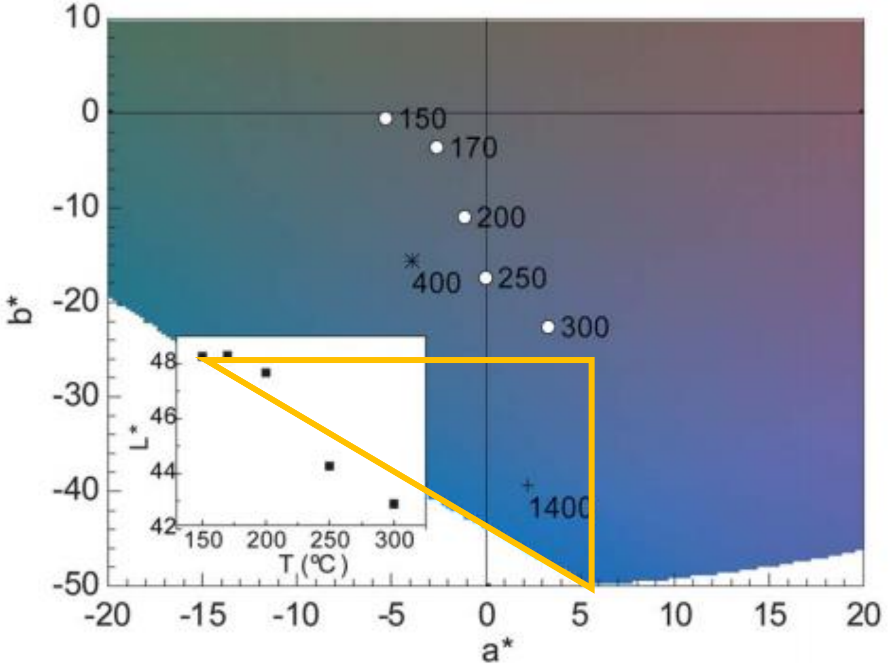

Fig. 6 *a***b** color space parameters of the synthesized samples (○) and nano-[26] (*) and micro-powder[36] (+) references. Labels correspond to the temperature of synthesis in °C. Background color shows an approximate representation of colors in the *a***b** region of interest for $L^* = 45$, obtained after a transformation of the $L^*a^*b^*$ space to the sRGB space using ref. 39. The inset shows the dependence of L^* with the temperature of synthesis.

Karmaoui et al. (2013). *Synthesis of cobalt aluminate nanopigments by a non-aqueous sol–gel route. Nanoscale, 5(10), 4277.* doi:10.1039/c3nr34229h

250ct parcel
3 years to assemble while living in situ
Photo and collection Geir Atle Gussiås

Mineral nomenclature

- $Mg^{2+}Al^{3+}{}_2O_4$ Spinel (stricto sensu)
- $(Mg^{2+},Co^{2+})Al^{3+}{}_2O_4$ Cobalt-bearing spinel
- $Co^{2+}Al^{3+}{}_2O_4$ Cobaltospinel
  (Cobalt aluminate)

- Vivid neon electric coveted "cobalt" blue

Sample	Formula
CoAl0.5	$^{T}(Co_{0.06}Mg_{0.70}Al_{0.24})^{M}(Co_{0.01}Mg_{0.23}Al_{1.76})O_4$
CoAl1	$^{T}(Co_{0.07}Mg_{0.69}Al_{0.23})^{M}(Co_{0.01}Mg_{0.22}Al_{1.77})O_4$
CoAl10	$^{T}(Co_{0.09}Mg_{0.68}Al_{0.23})^{M}(Co_{0.02}Mg_{0.21}Al_{1.77})O_4$
CoAl14	$^{T}(Co_{0.23}Mg_{0.55}Al_{0.22})^{M}(Co_{0.02}Mg_{0.20}Al_{1.78})O_4$
CoAl20	$^{T}(Co_{0.31}Mg_{0.48}Al_{0.21})^{M}(Co_{0.03}Mg_{0.18}Al_{1.79})O_4$
CoAl34	$^{T}(Co_{0.44}Mg_{0.37}Al_{0.19})^{M}(Co_{0.04}Mg_{0.15}Al_{1.81})O_4$
CoAl45	$^{T}(Co_{0.54}Mg_{0.30}Al_{0.17})^{M}(Co_{0.05}Mg_{0.11}Al_{1.83})O_4$
CoAl50	$^{T}(Co_{0.52}Mg_{0.27}Al_{0.21})^{M}(Co_{0.11}Mg_{0.10}Al_{1.79})O_4$
CoAl67	$^{T}(Co_{0.67}Mg_{0.17}Al_{0.16})^{M}(Co_{0.09}Mg_{0.08}Al_{1.84})O_4$
CoAl100	$^{T}(Co_{0.87}Mg_{0.00}Al_{0.13})^{M}(Co_{0.13}Mg_{0.00}Al_{1.87})O_4$

Note: T = tetrahedrally coordinated site; M = octahedrally coordinated site.

Bosi et al, American Mineralogist, Volume 97, pages 1834–1840, 2012

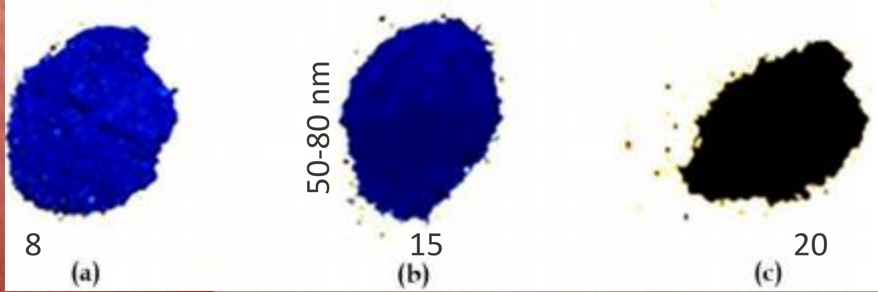

Rajabi, et al, *J Aust Ceram Soc* **55**, 219–227 (2019)

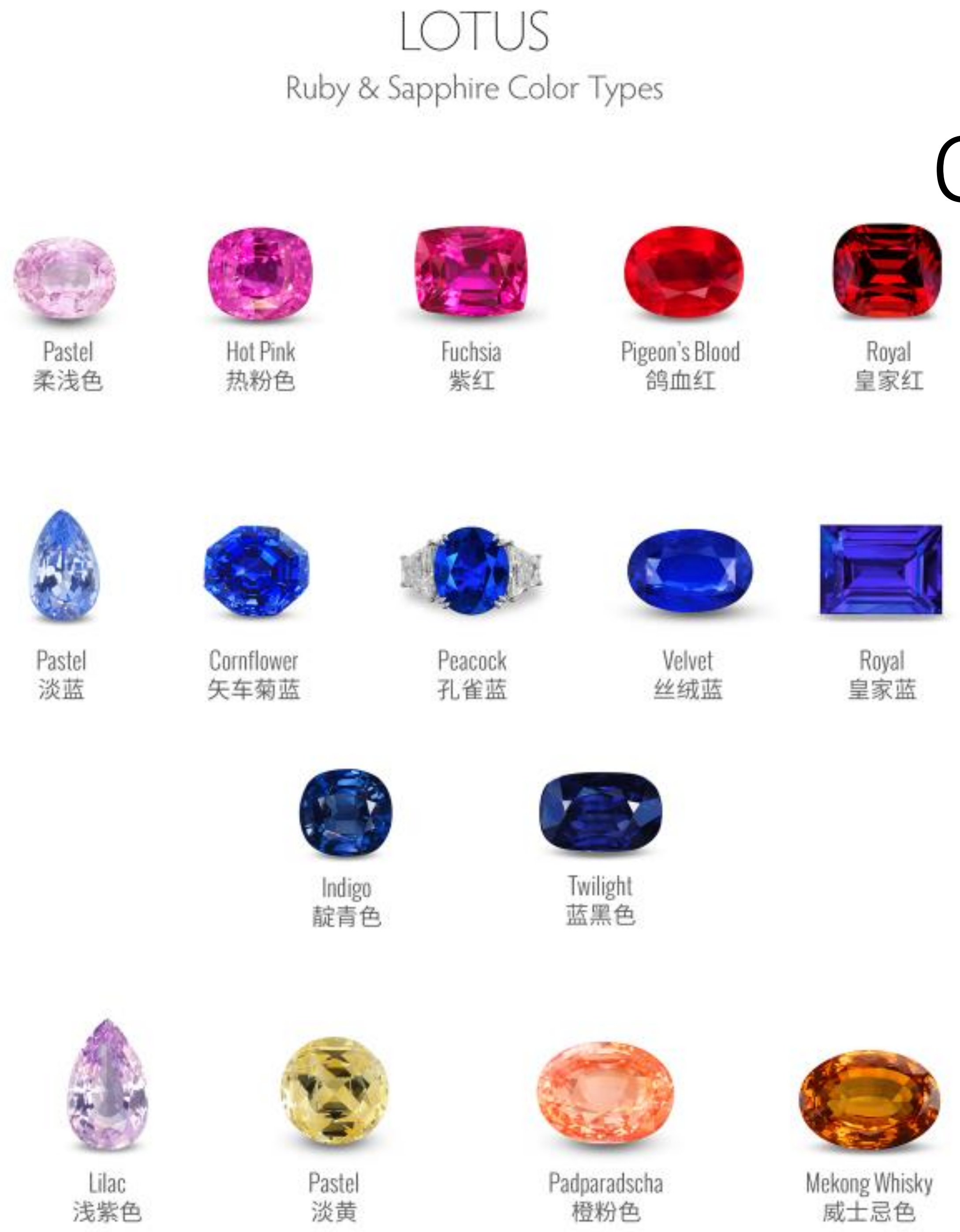

Overcoming nomenclature

- Colors in sapphires are not defined by the amount of Fe or Ti, nor a given ratio of (Cr+V)/Fe for rubies.
- No substitute for direct experience
- A "cobalt spinel" is about the glowing saturated neon blue perceived in person. The hype exist because of its incredible vividness, not because of an arbitrary ratio.

Blue spinels should lack non-blue chromophores

Tetrahedral [T]

$(Mg^{2+} Fe^{2+} Zn^{2+} {}_{Mn^{2+}} Co^{2+} {}_{Ni^{2+}} Al^{3+})_{\Sigma 1}$

Octahedral[M]

$(Al^{3+} {}_{Fe^{3+} Fe^{2+} V^{3+} Cr^{3+} Ti^{3+}} Mg^{2+} {}_{Co^{2+} Fe^{2+}})_{\Sigma 2}$

$Fe^{3+}Fe^{2+}$

$Fe^{3+}Fe^{2+}$

O_4

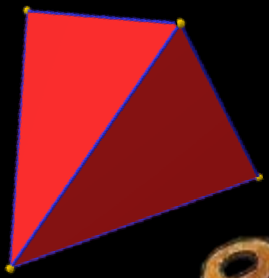

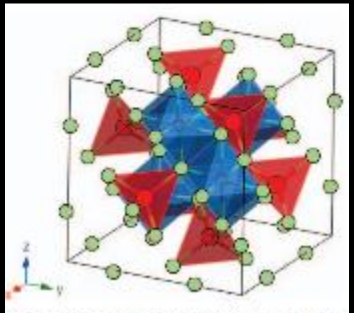

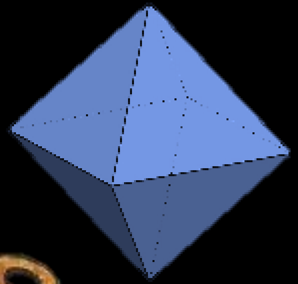

Fig. 1. Spinel structure, with the cubic unit cell outlined in black, oxygen ions in green, tetrahedra and T sites in red and octahedra and M sites in blue.

D'IPPOLITO et al, Mineralogical Magazine, October 2013, Vol. 77(7), pp. 2941–2953

Ore genesis triptic

- Source
  - Where do these element come from ?
  - How is aluminium hosted in carbonates ?

- Transport
  - Reconcentration of elements via a fluid

Deposition
  - Thermodynamic equilibrium

Pink octahedral spinel, Mogok, Ex Coll and photo N.HEBERT

Chauvire et al, Gems and Gemology 2015 DOI: 10.5741/GEMS.51.1.2

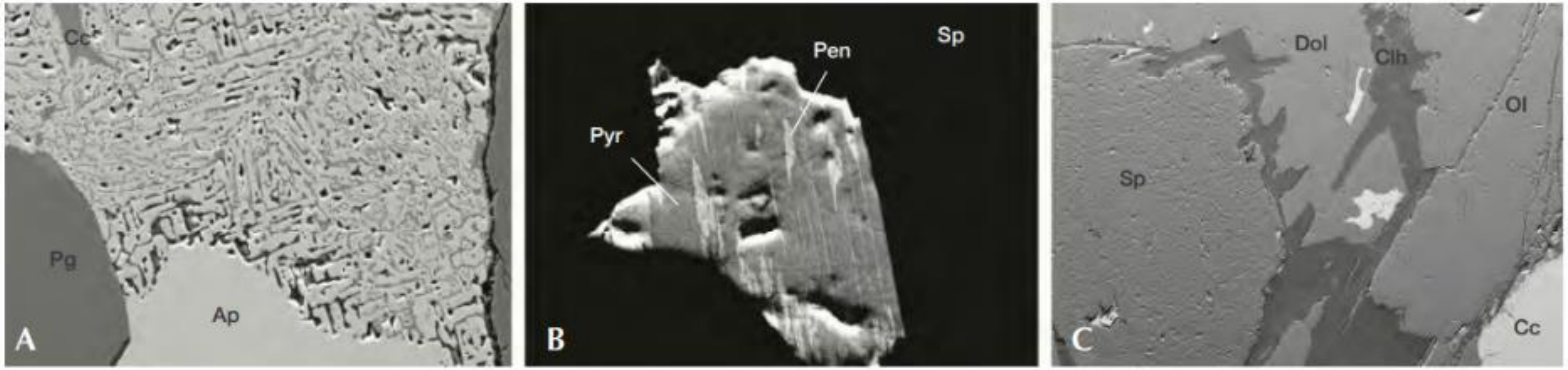

Figure 7. An inclusion of apatite in pargasite exhibits intergrowth with calcite (slightly magnesian; left, magnification 750×). In most cases, pyrrhotite inclusions have exsolutions of pentlandite, a sulfide with higher nickel content (center, magnified 1200×), which also contains cobalt. Using scanning electron microscopy with backscattered electron imaging, sensitive to the atomic number, a petrographic thin section of marble-bearing blue spinel shows that spinel and olivine are surrounded by clinochlore. The marble is composed of calcite and dolomite (right, magnified 65×). Ap = apatite, Cc = calcite, Clh = clinochlore, Dol = dolomite, Ol = olivine, Pen = pentlandite, Pg = pargasite, Pyr = pyrrhotite, Sp = spinel.

Fe/Co	867	562	1053	670	24
Species	Pyrrhotite	Pyrrhotite	Pyrrhotite	Pyrrhotite	Pyrite
Locality	Glencoe main	Soper River	Soper Falls	Soper Lk camp	Trailside
Lithology	Spl-bearing pod	Spl-bearing marble	Humitite	Spl-bearing marble	Spl-bearing silicate rock
Sample	2A-SPL-1	3A-1	3B	3C	3F-1 (after Spl)
n	4	3	3	5	1
Fe (wt.%)	60.99	61.79	63.19	60.32	43.06
Co	0.07	0.11	0.06	0.09	1.79
Ni	0.21	0.10	<0.03	0.04	<0.03
S	38.59	38.03	36.81	38.62	52.75
TOTAL	99.86	100.05	100.08	99.09	97.61

Below detection limit (wt.%): Mn (0.03), Zn (0.04).

What makes a deposit ?

Comparison of occurences

- An Phu/Luc Yen - Vietnam
- Baffin Island - Canada

255 photos of Spinel associated with Calcite	$CaCO_3$
96 photos of Spinel associated with Forsterite	Mg_2SiO_4
48 photos of Spinel associated with Clinohumite	$Mg_9(SiO_4)_4F_2$
40 photos of Spinel associated with Chondrodite	$(Mg,Fe^{2+})_5(SiO_4)_2(F,OH)_2$
33 photos of Spinel associated with Diopside	$CaMgSi_2O_6$
32 photos of Spinel associated with Phlogopite	$KMg_3(AlSi_3O_{10})(OH)_2$
25 photos of Spinel associated with Pargasite	$NaCa_2(Mg_4Al)(Si_6Al_2)O_{22}(OH)_2$

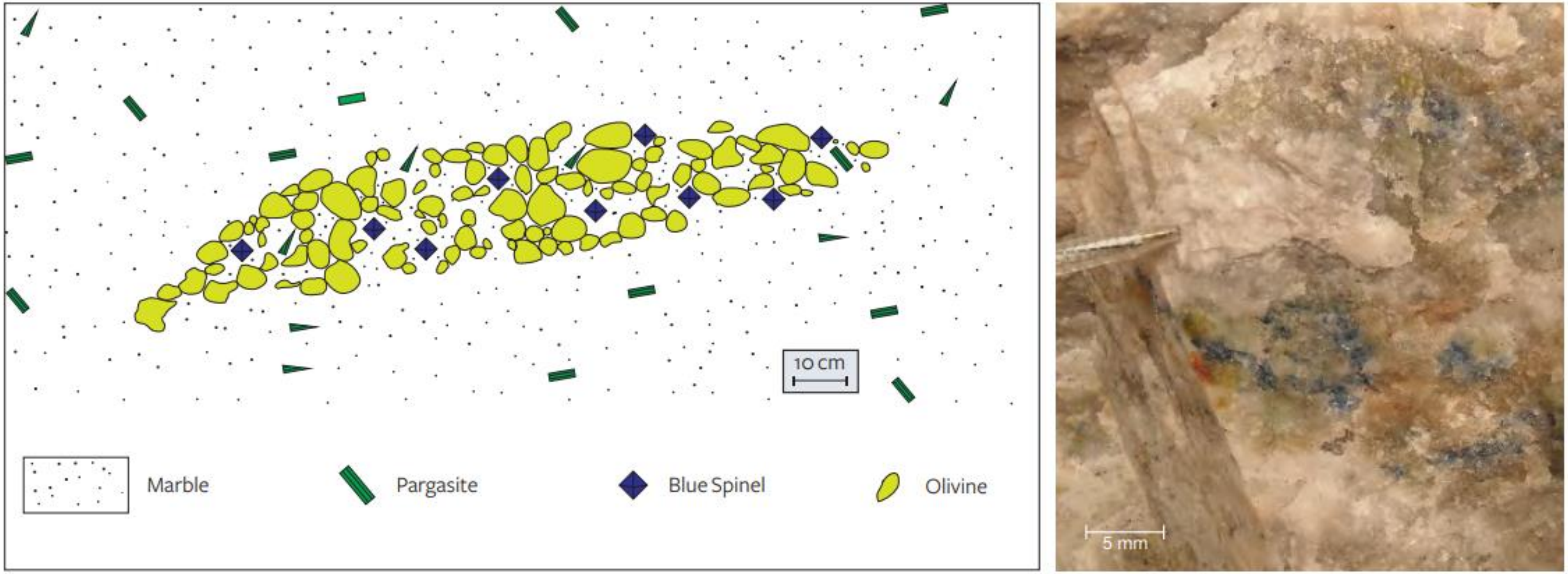

Figure 8. In Vietnam, primary blue spinel deposits appear as approximately lens-shaped bodies rich in olivine. These lenses are hosted in marble, and pargasite is found throughout the surrounding marble. Photo and drawing by Boris Chauviré.

Chauvire et al, Gems and Gemology · 2015
DOI: 10.5741/GEMS.51.1.2

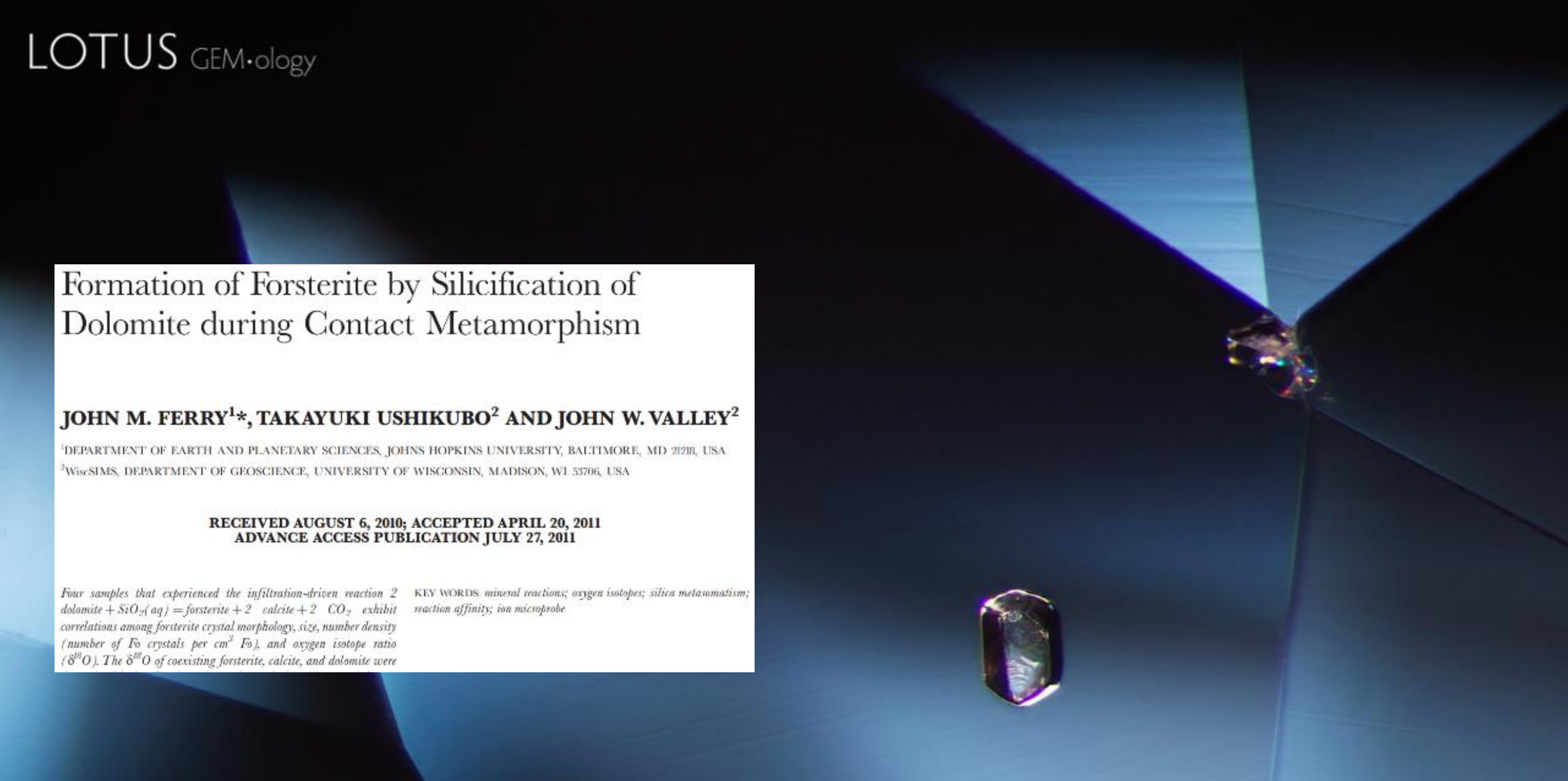

Formation of Forsterite by Silicification of Dolomite during Contact Metamorphism

JOHN M. FERRY[1]*, TAKAYUKI USHIKUBO[2] AND JOHN W. VALLEY[2]

[1]DEPARTMENT OF EARTH AND PLANETARY SCIENCES, JOHNS HOPKINS UNIVERSITY, BALTIMORE, MD 21218, USA
[2]WiscSIMS, DEPARTMENT OF GEOSCIENCE, UNIVERSITY OF WISCONSIN, MADISON, WI 53706, USA

RECEIVED AUGUST 6, 2010; ACCEPTED APRIL 20, 2011
ADVANCE ACCESS PUBLICATION JULY 27, 2011

Four samples that experienced the infiltration-driven reaction 2 dolomite + $SiO_2(aq)$ = forsterite + 2 calcite + 2 CO_2 exhibit correlations among forsterite crystal morphology, size, number density (number of Fo crystals per cm^3 Fo), and oxygen isotope ratio ($\delta^{18}O$). The $\delta^{18}O$ of coexisting forsterite, calcite, and dolomite were

KEY WORDS: *mineral reactions; oxygen isotopes; silica metasomatism; reaction affinity; ion microprobe*

This Sri-lankan blue spinel is home to a tiny, well-formed forsterite crystal identified with micro Raman.
Photographer: E. Billie Hughes • Image Number: A-003-6581-1 • Field of View = 3 mm • Date Posted: 15 July 2020
Gübelin, E.J. and Koivula, J.I. (2005) Photoatlas of Inclusions in Gemstones, Volume 2. Basel, Switzerland, Opinio Publishers, 830 pp.; RWHL*.

$$\mathrm{Fo} + 2\ \mathrm{Cal} + 3\ \mathrm{SiO_2(aq)} = 2\ \mathrm{Di} + 2\ \mathrm{CO_2}.$$

Small diopside crystal (confirmed with micro Raman) in this blue spinel from Madagascar.
Photographer: E. Billie Hughes • Image Number: A-003-6579-1 • Field of View = 2 mm • Date Posted: 15 July 2020
Gübelin, E.J. and Koivula, J.I. (2005) Photoatlas of Inclusions in Gemstones, Volume 2. Basel, Switzerland, Opinio Publishers, 830 pp.; RWHL*.

LOTUS GEM·ology

RAITH J. metamorphic Geol., 2008, 26, 647–667
doi:10.1111/j.1525-1314.2008.00779.x

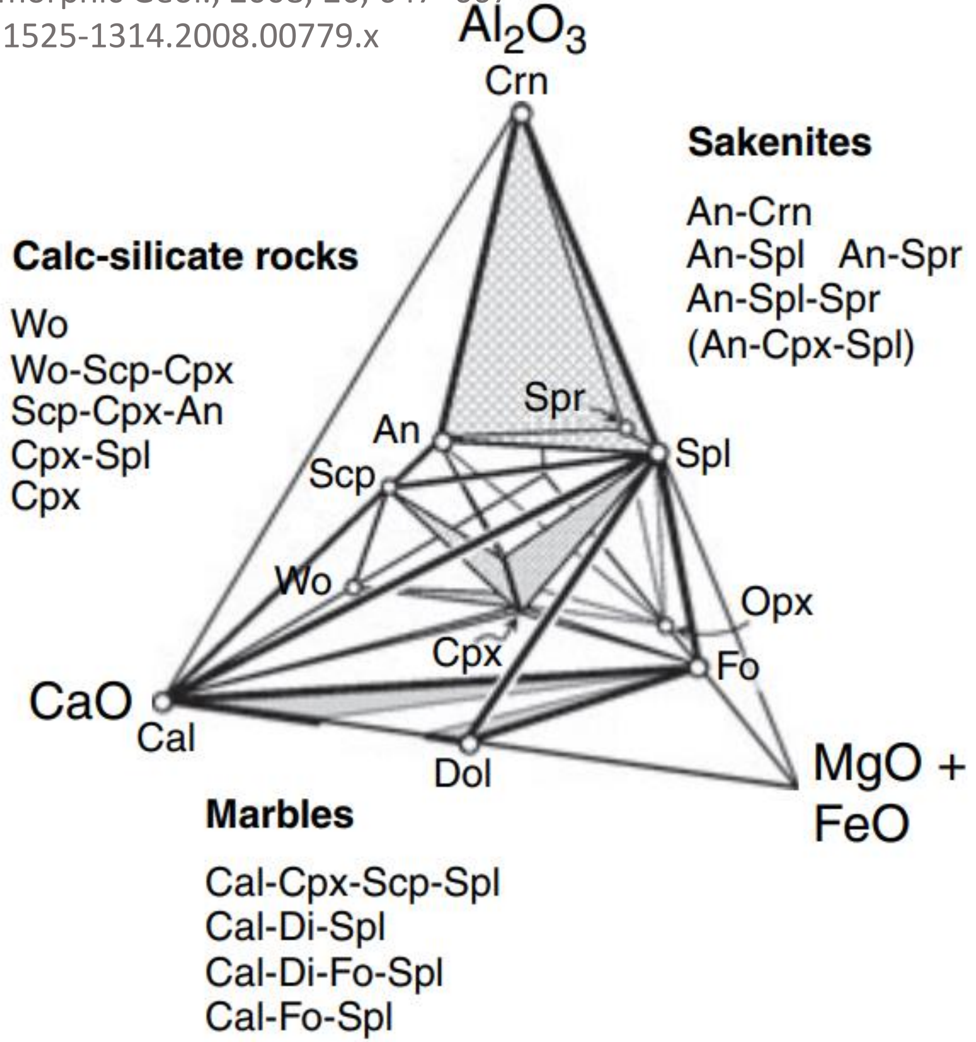

Fig. 5. CaO-MgO + FeO-Al_2O_3-SiO_2 tetrahedron illustrating schematically the relationship between bulk chemistry and mineral assemblages of sakenites and the marble-calcsilicate-skarn association in the Androyan terrane of southern Madagascar. The phase relations correspond to *P–T* conditions of ~800 °C, 5–6 kbar and $X_{CO_2} > 0.8$.

Blue spinel, sapphirine, anorthite, scapolite, Ambarano, Beraketa, Madagascar Coll N.HEBERT

Petrological assemblage in BAFFIN ISLAND, NUNAVUT, CANADA

Cobalt-blue spinel outcrop at the Qila occurrence:
[3E-1] Calc-silicate pod;
[3E-2] Pargasite-calcite rock;
[3E-3] Marble.

Next slide :
Vivid blue spinel with white carbonate in calc-silicate rock composed of green pargasite with subordinate greyish scapolite.

Qila occurrence, Kimmirut area.

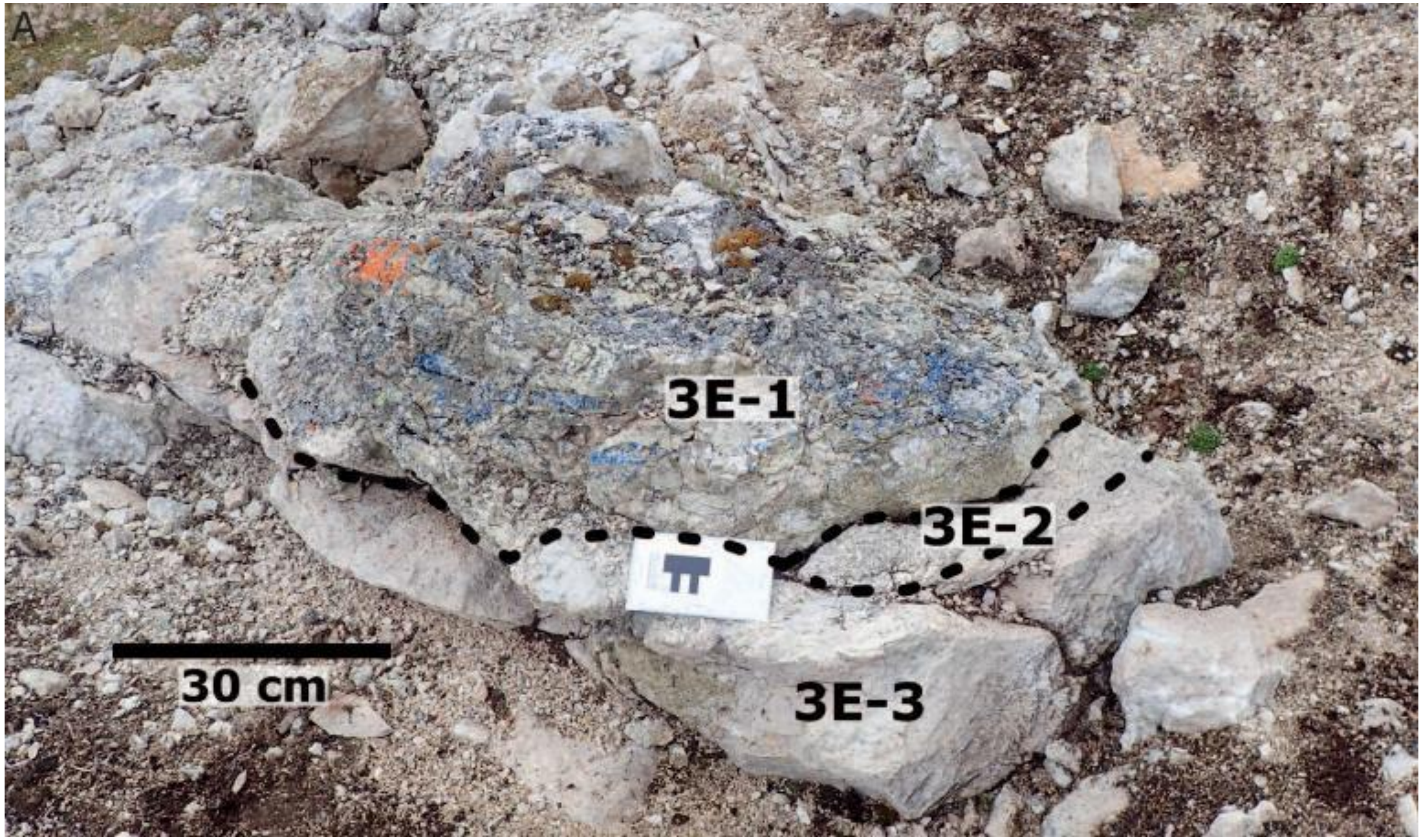

M.Belley et al, The Canadian Mineralogist Vol. 57, pp. 147-200 (2019) DOI:10.3749/canmin.1800060

M.Belley et al, The Canadian Mineralogist Vol. 57, pp. 147-200 (2019) DOI:10.3749/canmin.1800060

Petrological assemblage

- Silicate-rich spinel-bearing rock
- Predominant spinel-bearing unit at the Trailside occurrence, Kimmirut area.
- Composed of:
  - fine-grained muscovite (Ms) pseudomorphs after an unknown mineral
  - coarse-grained phlogopite (Phl),
  - calcite (Cal),
  - spinel (Spl)

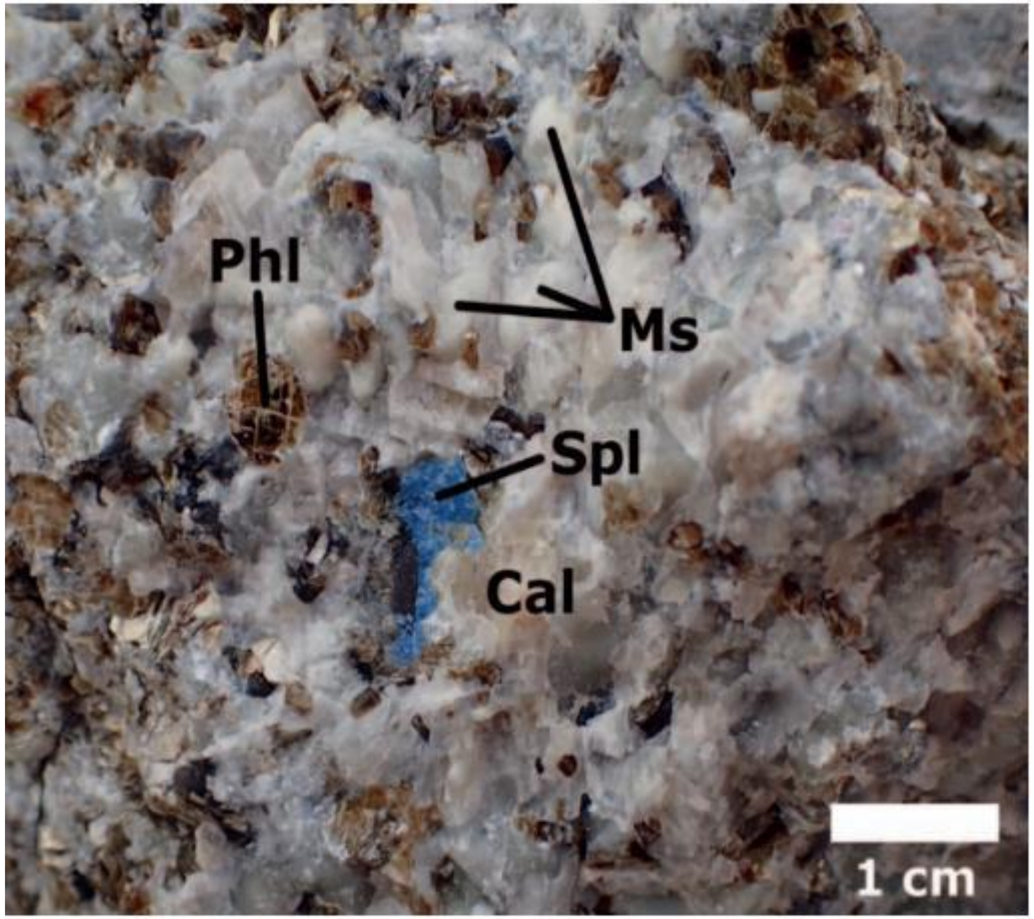

M.Belley et al, The Canadian Mineralogist Vol. 57, pp. 147-200 (2019) DOI:10.3749/canmin.1800060

Mineralogy of micas : role of K in

- F-rich aspidolite (Na phlogopite) known in Luc Yen
- Phlogopite ($KMg_3AlSi_3O_{10}(F, OH)_2$) & muscovite known in Mogok & Luc Yen

Purple spinel with mica, Cong Troi, An Phu, Luc Yen, Coll N.HEBERT

Blue spinel and phlogopite, Khe Khi, An Phu, Luc Yen, Coll N.HEBERT

Deciphering fluid inclusions

- The metamorphic fluid system was rich in:
  - CO_2 released from devolatilisation of carbonates
  - fluorine, chlorine and boron released by molten salts ($NaCl$, KCl, $CaSO_4$)
- Evaporites are key to explaining the formation of these deposits.

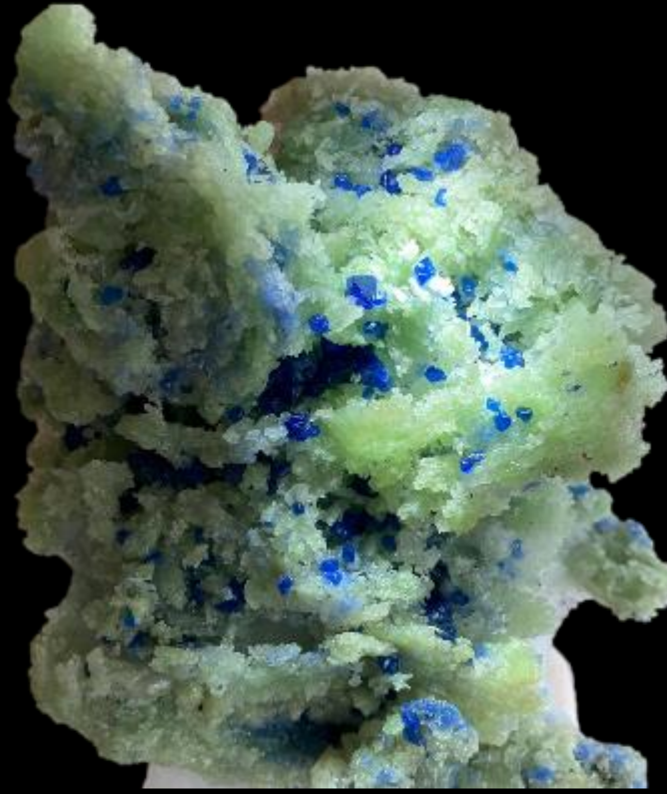

Specimen and picture : Hứa Toàn

Deciphering fluid inclusions

- **Unusual chemistry of CO_2 – H_2S – COS – S_8 –AlO(OH) bearing fluids**

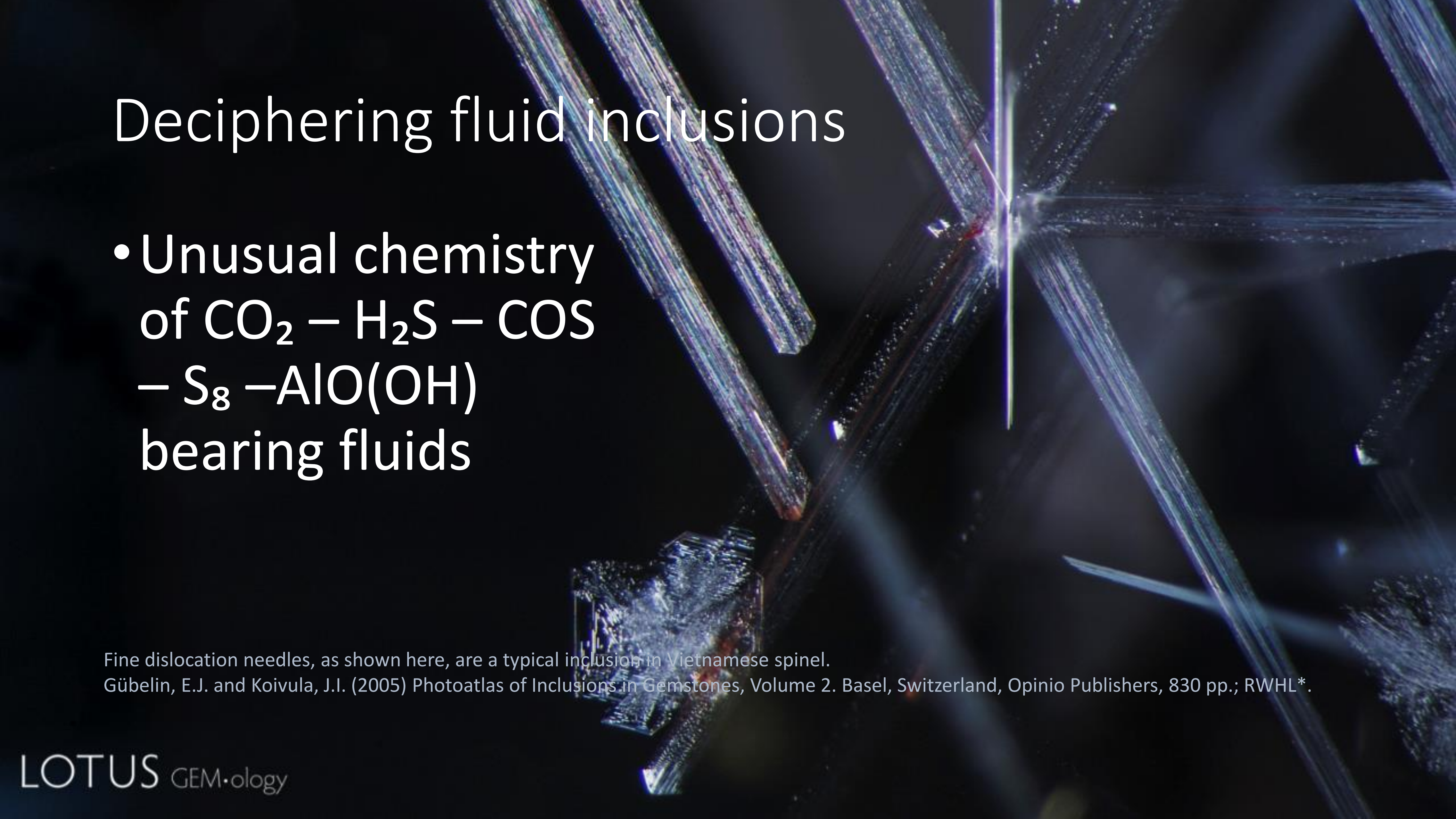

Fine dislocation needles, as shown here, are a typical inclusion in Vietnamese spinel.
Gübelin, E.J. and Koivula, J.I. (2005) Photoatlas of Inclusions in Gemstones, Volume 2. Basel, Switzerland, Opinio Publishers, 830 pp.; RWHL*.

TABLE 6C. ESTIMATED PROTOLITH COMPOSITION OF METACARBONATE SAMPLES FROM SOPER RIVER AND QILA, KIMMIRUT AREA

Locality		Soper River	Soper River	Qila	Qila	Qila	Qila	Qila (area)
Lithology		Lapis lazuli	Lapis lazuli	Calc-silicate	Prg-Cal rock	Spl-bearing marble	Phl-richer, Spl-poor marble	Marble
Sample		3A-LAPIS-1	3A-LAPIS-2	3E-1	3E-2	3E-3-A	3E-3-B	3E-M2
Siliciclastic contribution [a] (wt.%)	Al/Si (g/g)	0.34	0.33	0.4	0.44	0.15	0.15	0.16
	CaO	2.48	2.93	2.84	1.84	0.51	0.55	0.37
	MgO	1.29	1.48	1.65	1.16	0.15	0.17	0.11
	Na_2O	0.52	0.59					
Original H_2O estimate (wt.%) [b]	H_2O	2.61	2.91	3.58	2.67	0.15	0.17	0.12
Original carbonate [c]	CaO	21.62	16.32	10.06	24.16	42.49	45.75	47.63
	MgO	6.87	8.72	13.35	12.59	11.35	7.99	7.22
Original carbonate	CO_2	24.46	22.34	22.46	32.71	45.73	44.64	45.26
Original evaporite [d]	Na	4.31	4.73					
	Cl	6.65	7.29					
Total [e]		119.38	123.92	114.45	116.93	109.47	109.12	107.92
Carbonate species (mol.%)	Magnesite	0	0	46	0	0	0	0
	Dolomite	44	74	54	72	37	24	21
	Calcite	56	26	0	28	63	76	79
		Original rock composition (wt.%) [f]						
Siliciclastic	Sand	8	10.6	4.2		6.3	6.7	4.7
	Mud	38	41	55.5	39.1	2.7	3.1	2.4
	Clay				1.4			
	Sili. Total	46	51.5	59.6	40.5	9	9.7	7.1
Carbonate		44.7	38.7	40.4	59.5	91	90.3	92.9
Halite		9.3	9.8					

Locality		Trailside	Trails. (area)	Trails. (area)	Trailside	Trailside	Trailside (area)	Trailside (area)
Lithology		Spl-bearing silicate rock (Spl-poor)	Marble	Marble	Cal-Phl-Spl rock	Diopsidite	Diopsidite	Diopsidite
Sample		3F-1	3F-M1	3F-M2	3F-2	3F-4	3F-CS2	3F-CS3
Siliciclastic contribution [a] (wt.%)	Al/Si (g/g)	0.73	0.24	0.27	0.72	0.04	0.1	0.18
	CaO	0.32	0.62	0.27	0.21	2.79	3.45	3.24
	MgO	0.45	0.25	0.12	0.3	0.59	0.86	1.08
	Na_2O							
Original H_2O estimate (wt.%) [b]	H_2O	2.93	0.4	0.21	1.93	0	0.42	1.35
Original carbonate [c]	CaO	15.28	42.78	49.83	21.19	20.71	16.5	13.31
	MgO	7.63	8.77	2.94	16.05	15.71	15.34	17.07
Original carbonate	CO_2	20.32	43.15	42.32	34.16	33.41	29.71	29.08
Original evaporite [d]	Na							
	Cl							
Total [e]		107.05	108.79	101.43	116.54	125.68	123.71	124.97
Carbonate species (mol.%)	Magnesite	0	0	0	5	5	23	44
	Dolomite	69	29	8	95	95	77	56
	Calcite	31	71	92	0	0	0	0
		Original rock composition (wt.%) [f]						
Siliciclastic	Sand		5.4	2.1		44.4	43.5	31.2
	Mud		7.5	4			6.7	21.2
	Clay	7.2			7.3			
	Sili. Total	52.3			31.3			
Carbonate		59.5	12.9	6.1	38.6	44.4	50.2	52.4
Halite		40.5	87.1	93.9	61.4	55.6	49.8	47.6

[a] Estimated based on reference averages and samples of modern sedimentary rocks (see text).
[b] Assuming 5 wt.% water in shales and claystones.
[c] Siliciclastic contribution subtracted from whole rock total.
[d] Siliciclastic contribution subtracted from whole rock total, for lapis lazuli only, assuming all excess Na is halite.
[e] Whole rock composition excluding volatiles and with the addition of the estimated original CO_2, H_2O, and where applicable, Cl.
[f] Where the siliciclastic proportion is calculated assuming it contains all Al, Si, Ti, Cr, K, Na (except in lapis lazuli), and their calculated estimated contribution of Ca and Mg; and the carbonate proportion contains the remainder of Ca and Mg plus CO_2.

M.Belley et al, The Canadian Mineralogist Vol. 57, pp. 147-200 (2019) DOI:10.3749/canmin.1800060

Origin of the protolith

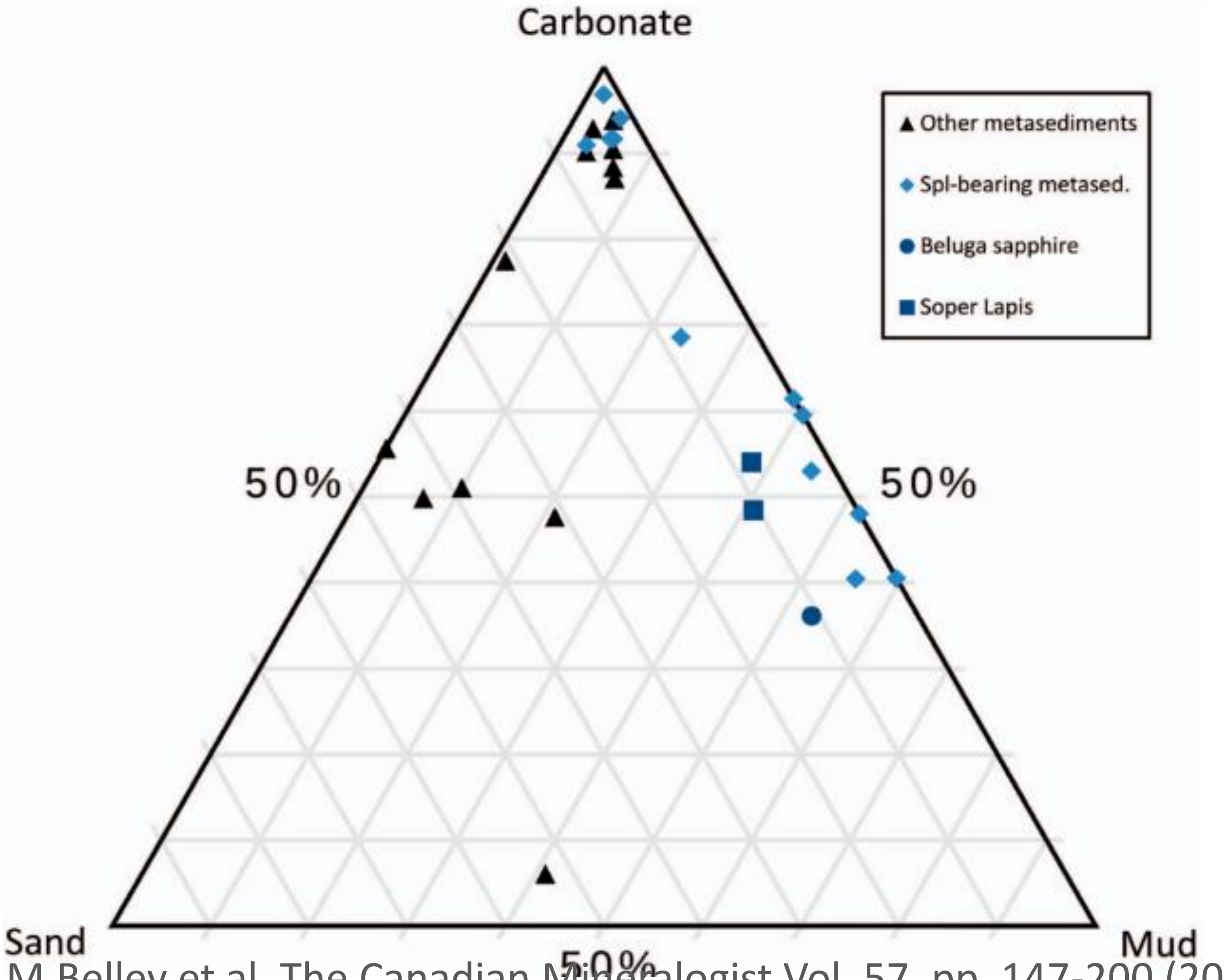

M.Belley et al, The Canadian Mineralogist Vol. 57, pp. 147-200 (2019) DOI:10.3749/canmin.1800060

Age of Marble-hosted spinel deposits

- Miocene at Hunza

(**10.8** ± 0.3 to 5.4 ± 0.3 Ma)

- Miocene at Mogok

(**18**.7 ± 0.2 to 17.1 ± 0.2 Ma)

- Eocene at Luc Yen

(**38**.1 ±0.5 Ma age zircon in ruby)

- Paleoproterozoic at Baffin Island

(**1820-1850** Ma)

Mineralization occurring while ductile deformation was active in peak metamorphic conditions in the Red River shear zone

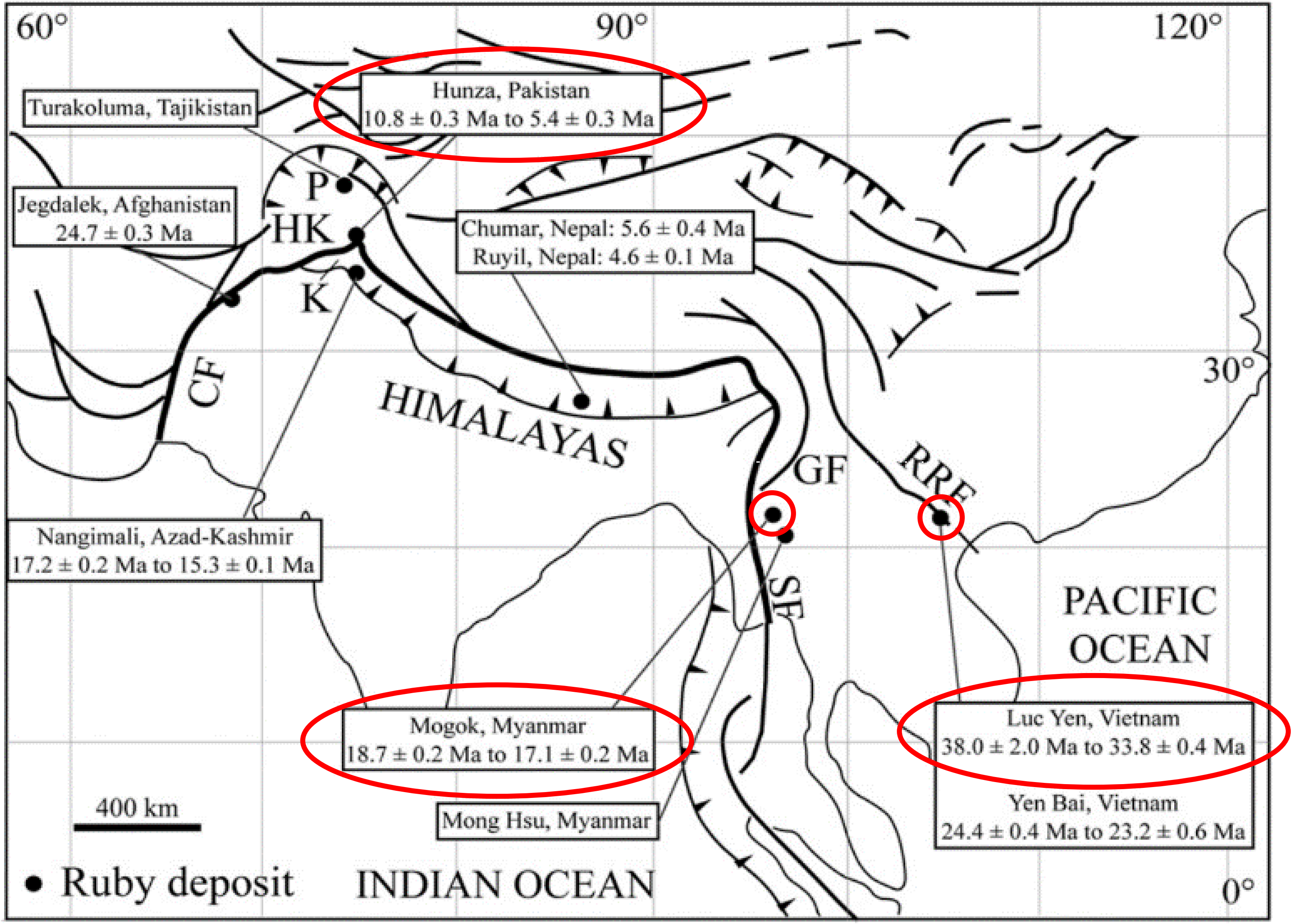

V. Garnier et al. Ore Geology Reviews 34 (2008) 169–191

Occurences

- Structural control

Chauvire et al, Gems and gemology, 2015

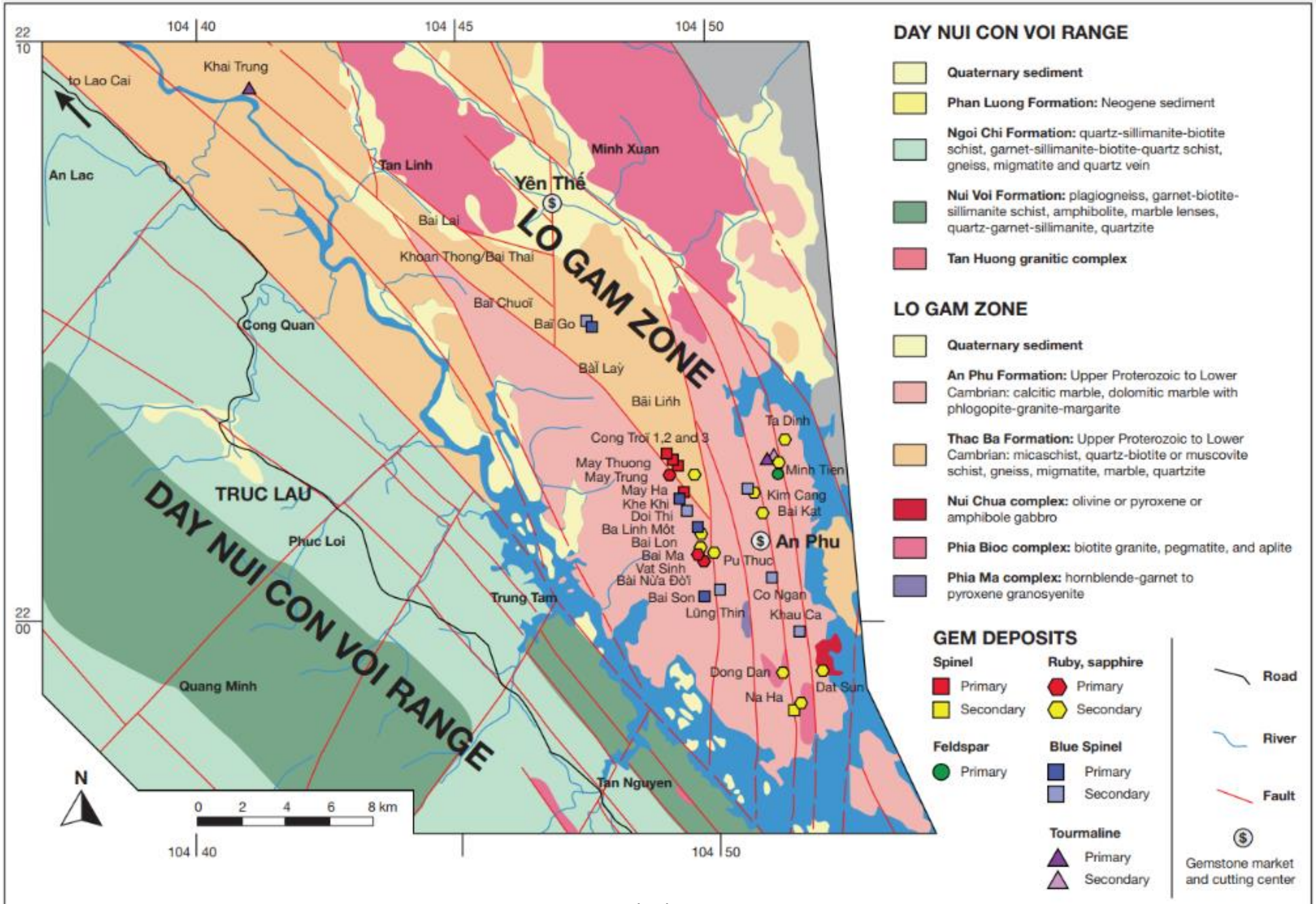

Van Long et al, Gems and gemology, 2013 (w), pp 233-245

- Temperatures are between 630 and 745 °C for the respective mines of Minh Tien (630 ° C), Bai Da Lan (675 – 700 ° C), **An Phu (690 ° C),** and Nuoc Ngap (745 ° C).

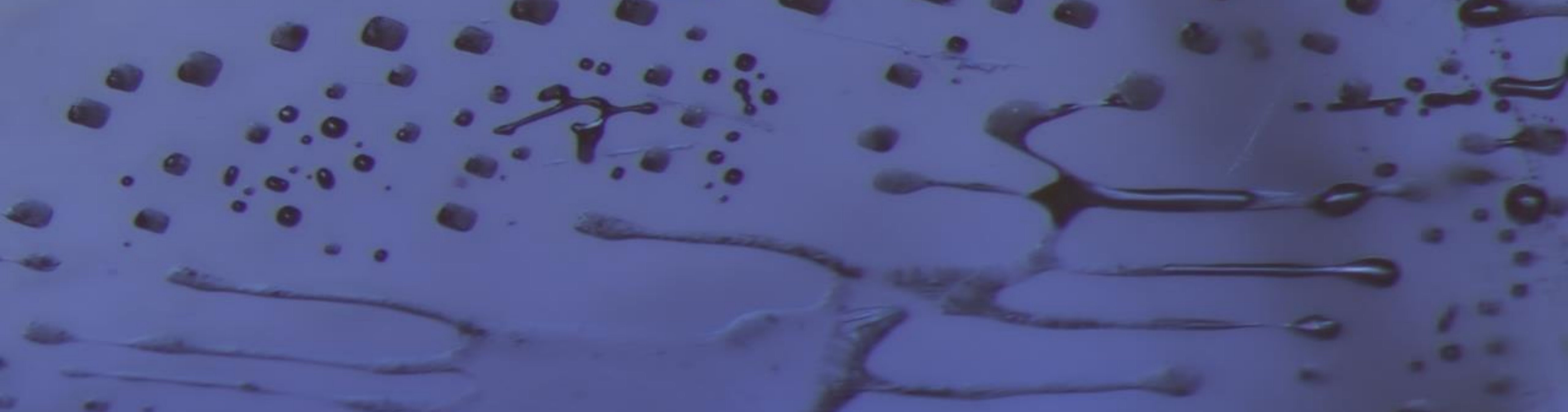

Melted fingerprints showing heat altered octahedra give evidence of heat treatment in this cobalt diffused spinel.
Natural Spinel • No Origin • Enhancements: Heat + Diffusion of external coloring agents (H-D); Heat + Fissure Healing (H-FH) • Photo: E. Billie Hughes
• Saeseaw, S., Wang, W. et al. (2009) Distinguishing Heated Spinels from Unheated Natural Spinels and from Synthetic Spinels. GIA, 13 pp.; RWHL.

Geochemical control sum-up

- Thermal reduction of evaporite by organic matter
- High temperature-medium pressure metamorphism of platform carbonates

Preservation of the spinel

- Strong redissolution
- Sometimes followed by recrystalisation
- Result in oriented growth
- Influence of nucleation

Blue spinel, Khe Khi, Luc Yen, Coll and photo N.HEBERT

Litterature

- “Spinel heaven” group https://www.facebook.com/groups/852689831572585
- Philippe M. Belley∗ , Lee A. Groat Ore Geology Reviews Volume 116, January 2020, 103259 https://doi.org/10.1016/j.oregeorev.2019.103259
- V. D'Ippolito; et al Mineralogical Magazine (2013) 77 (7): 2941–2953. https://doi.org/10.1180/minmag.2013.077.7.05
- D’Ippolito, V., Andreozzi, G.B., Hålenius, U. et al. Color mechanisms in spinel: cobalt and iron interplay for the blue color. Phys Chem Minerals 42, 431–439 (2015).
- Chauvire et al, Gems and Gemology · 2015 DOI: 10.5741/GEMS.51.1.2
- V. Garnier et al. Ore Geology Reviews 34 (2008) 169–191
- A.Palke GIA https://youtu.be/kU4bZRmIKp4
- Van Long et al, Gems and gemology, 2013 (w), pp 233-245
- Muhlmeister et al, Gems and gemology 2013,81-98
- Andreozzi et al, *Phys Chem Minerals* **46,** 343–360 (2019). https://doi.org/10.1007/s00269-018-1007-5
- Le Thi Thu Huong, Vietnam Journal of Earth Sciences, 40(1), 47-55, Doi:10.15625/0866-7187/40/1/10915
- Karmaoui et al. (2013). *Synthesis of cobalt aluminate nanopigments by a non-aqueous sol–gel route. Nanoscale, 5(10), 4277.* doi:10.1039/c3nr34229h
- Bosi et al, American Mineralogist, Volume 97, pages 1834–1840, 2012
- Rajabi, et al, *J Aust Ceram Soc* **55,** 219–227 (2019)
- F. LIN SUTHERLAN Mineralogical Magazine, August 1996, Vol. 60, pp. 623-638
- RAITH J. metamorphic Geol., 2008, 26, 647–667 doi:10.1111/j.1525-1314.2008.00779.x
- Lenaz et al, Periodico di Mineralogia, ECMS 2015, 111-112

If you have any question, please contact me through social media or n.hebert.geo@gmail.com

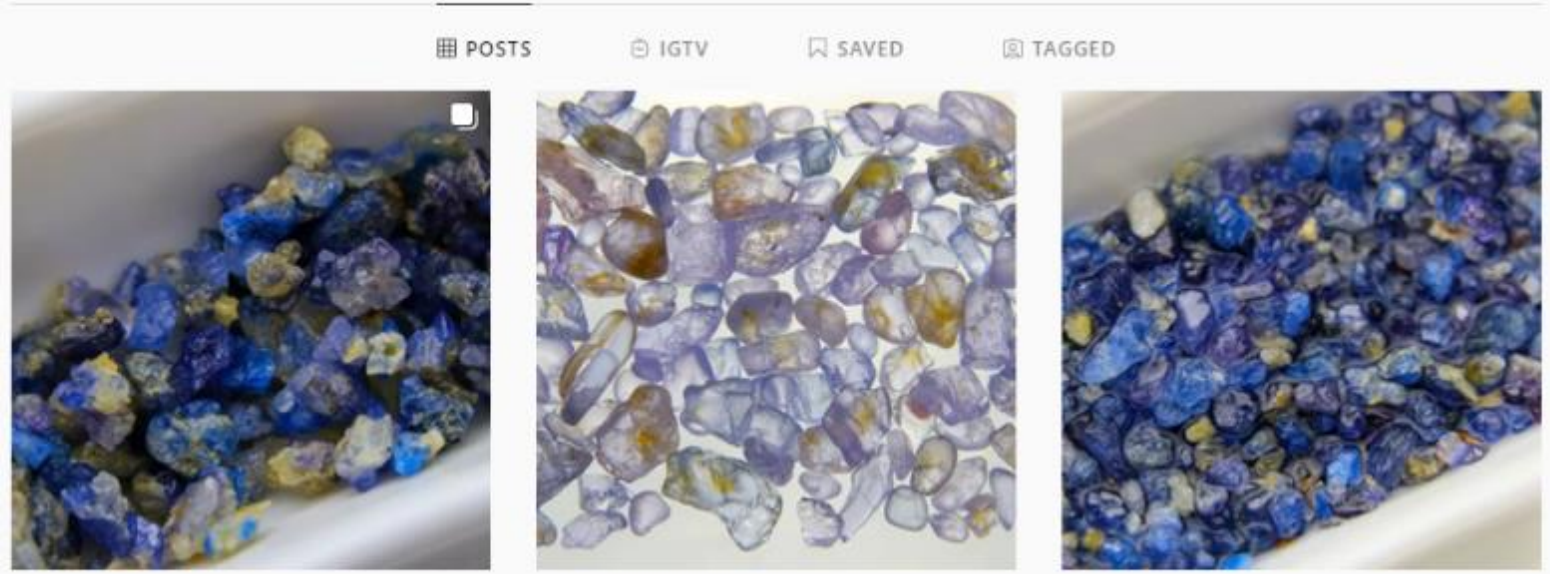

Trace elements

Spinels from **Cong Troi** have:

low to extremely **low Zn (< 500 ppm)**

high Fe contents (3,000 to 16,000 ppm)

while those from **An Phu area are Zn-rich (up to 11,000 ppm).**

Iron is the dominant element for the other colored spinels whereas Zn, Cr and V contents are extremely variable.

The Bai Son blue spinel is Fe-rich (5,000 to 7,200 ppm) with some V (950 to 1,830 ppm), Cr (270 to 480 ppm), Co (240 to 400 ppm) and Ni (550 to 950 ppm).

Occurrences I won't talk about

- Crazy Sphinx Mine, Helena, Helena Mining District, Lewis and Clark Co., Montana, USA
- Lime Crest Quarry, Franklin Marble, Sparta Township, Sussex County, New Jersey, USA
- Canta Galo mine, Nova Era, Minas Gerais, Brazil
- Toal dei Rizzoni, San Giovanni di Fassa, Trento Province, Trentino-Alto Adige, Italy
- Mustio quarry, Raseborg, Uusimaa, Finland
- Ladjuar Medam, Sar-e Sang, Koksha Valley, Khash & Kuran Wa Munjan Districts, Badakhshan, Afghanistan
- White Cutting, Slyudyanka, Lake Baikal area, Irkutsk Oblast, Russia
- Antanimora Sud, Ambovombe-Androy, Androy, Madagascar
- Ampandrandava phlogopite mine, Beraketa, Bekily, Androy, Madagascar
- Tuléar Province, Madagascar
- Jemaa, Kaduna, Nigeria
- Kajiado County, Kenya

https://www.mindat.org/photo-285544.html E.C Graff Specimen and picture

TABLE 2D. COMPOSITION OF SPINEL FROM QILA AND TRAILSIDE, KIMMIRUT AREA

Locality	Qila		Qila		Qila		Qila (area)		Trailside		Trailside	
Lithology	Spl-bearing calc-silicate		Prg-Cal rock		Spl-bearing marble		Dolomitic marble		Spl-bearing silicate rock		Cal-Phl-Spl rock	
Color	Cobalt-blue		Sky blue		Cobalt-blue		Light violet		Cobalt-blue		Cobalt-blue	
Sample	3E-1		3E-2		3E-3-A		3E-M1		3F-1		3F-2	
n	5	σ	4	σ	3	σ	4	σ	4	σ	4	σ
TiO_2 (wt.%)	<0.01	0	<0.01		<0.01		0.02	0	<0.01	0	<0.01	0
ZnO	0.16	0.01	0.05	0	0.05	0.02	0.09	0.01	0.05	0.02	0.13	0.02
Al_2O_3	71.39	0.26	71.75	0.04	72.42	0.23	71.72	0.23	70.84	0.27	70.56	0.25
V_2O_3	<0.02		<0.02	0	<0.02		0.04	0.02	<0.02		<0.02	
Cr_2O_3	<0.03		<0.03		0.04	0.01	<0.03		<0.03		<0.03	
FeO	3.55	0.11	2.25	0.03	2.45	0.07	1.64	0.06	5.20	0.09	5.12	0.02
CoO	0.07	0.01	0.03	0.02	0.03	0.01	<0.03		0.06	0.01	0.06	0.01
NiO	0.04	0.01	<0.03		0.03	0.02	<0.03		<0.03		<0.03	
MnO	0.05	0.02	0.04	0.01	0.03	0.01	0.03	0.02	0.06	0.02	0.06	0.01
MgO	24.78	0.17	26.62	0.21	25.57	0.03	26.82	0.04	23.62	0.08	23.65	0.19
TOTAL	100.04		100.74		100.62		100.36		99.83		99.58	
Ti (*apfu*)	bdl		bdl		bdl		0.003		bdl			
Zn	0.023		0.007		0.007		0.013		0.007		0.019	
Al	16.184		16.059		16.223		16.070		16.199		16.180	
V	bdl		bdl		bdl		0.006		bdl		bdl	
Cr	bdl		bdl		0.006		bdl		bdl		bdl	
Fe	0.571		0.357		0.389		0.261		0.844		0.833	
Co	0.011		0.005		0.005		bdl		0.009		0.009	
Ni	0.006		bdl		0.005		bdl		bdl		bdl	
Mn	0.008		0.006		0.005		0.005		0.010		0.010	
Mg	7.106		7.536		7.246		7.601		6.832		6.860	

Normalized to 32 oxygen atoms per formula unit. bdl – below detection limit

M.Belley et al, The Canadian Mineralogist Vol. 57, pp. 147-200 (2019) DOI:10.3749/canmin.1800060

- Most spinel occurrences on Baffin Island are interpreted to have dolomitic limestone and dolomitic marl protoliths that are consistent with typical non-evaporitic platform sediments transformed by subsequent
- Evaporitic rocks typically have high Mg contents and relatively low Fe (caused by the widespread occurrence of Mg-rich clays), and evaporitic argillites are characterized by high K, Li, F, and B contents
- The abundance of Mg relative to Ca at most spinel occurrences is adequately explained by diagenetic dolomitization and does not imply an evaporitic origin

M.Belley et al, The Canadian Mineralogist Vol. 57, pp. 147-200 (2019) DOI:10.3749/canmin.1800060

- Spinel-bearing rocks in Baffin Island are richer than expected in B, F, and Cl.
- High F and Cl contents reflect the presence of pargasite, phlogopite, humite, and/or scapolite.
- These elements are highly mobile and may not be representative of the protolith.
- Indeed, an increased incorporation of F and Cl relative to OH in phlogopite, pargasite, and humite could be explained by greater pore fluid salinity at high grades of metamorphism.

M.Belley et al, The Canadian Mineralogist Vol. 57, pp. 147-200 (2019) DOI:10.3749/canmin.1800060

- The presence of evaporites at most spinel occurrences is therefore unlikely, and evaporites are not genetically related to gem spinel
- Metamorphism of a protolith with the correct proportions of major elements, which occur in typical non-evaporitic carbonate platform sedimentary rocks, is the only criteria.

- The relative abundances of Al and Si appear to be an important control on whether spinel will form; calc-silicate rocks with low Al/Si are at best Si saturated (no Si-undersaturated phases such as Al oxides, forsterite, ha¨uyne; e.g., sulfide-rich diopsidite at Glencoe Island), and at worst are Si oversaturated (e.g., quartz-bearing diopsidite near Trailside).
- Most calc-silicate rocks have low K/Al molar fractions. If not, they are likely to express phlogopite
- Potassium activity doesn’t control whether or not spinel occurs.
- The dominant geochemical control on spinel genesis in magnesian calc-silicate rocks under P-T conditions of granulite facies, ie 810 8C and 8.0 kbar appears to be the abundance of Si relative to Al.
- In contrast to calc-silicate rocks, spinel-bearing and spinel-absent marbles overlap in Al/Si and Ca/Mg ratios, but differ significantly in K/Al molar ratios.
- Spinel-bearing marbles are all very poor in K, while other marbles have K/Al ’ 1 (Fig. 28B). Phlogopite is a common constituent of spinel-bearing assemblages, which can include forsterite, diopside, and pargasite. The proportions of these minerals are expected to obey the following equilibrium reactions: 3 Di þ Spl þ 2 Dol þ 2 Kþ ðaqÞ þ 4ð Þþ H2O; F CO2 $ 2 Phl þ 5 Cal ð1Þ 6 Fo þ Spl þ 7 Cal þ 2 Kþ ðaqÞ þ 4ð Þþ H2O; F 7 CO2 $ 2 Phl þ 7 Dol ð2Þ 6 Prg þ 3 Spl þ 9 Dol þ 12 Kþ ðaqÞþ12 Hð Þ 2O; F þ 3 CO2 $ 12 Phl þ 21 Cal ð3Þ In all three reactions, low K activity would favor spinel over phlogopite. The forsterite-spinel marbles contain sufficient calcite for the reaction to proceed, and thus K could be a limiting reactant preventing complete incorporation of Al into phlogopite. Similarly, in some phlogopite-bearing marbles and in Qila calc-silicate rock, dolomite, pargasite, and spinel occur as a stable assemblage, leaving low K activity as a potential limiting factor in the phlogopite-forming reaction. The predominance of Na over K in the pargasites indicates an Na-dominant fluid composition and reinforces the low-K hypothesis. At Spinel Island, spinel-, phlogopite-, and calcite-bearing diopsidite

M.Belley et al, The Canadian Mineralogist Vol. 57, pp. 147-200 (2019) DOI:10.3749/canmin.1800060

- Most calc-silicate rocks have low K/Al molar fractions. If not, they are likely to express phlogopite
- Potassium activity doesn’t control whether or not spinel occurs.
- The dominant geochemical control on spinel genesis in magnesian calc-silicate rocks under P-T conditions of granulite facies, ie 810 8C and 8.0 kbar appears to be the abundance of Si relative to Al.
- In contrast to calc-silicate rocks, spinel-bearing and spinel-absent m but differ significantly in K/Al molar ratios.
- Spinel-bearing marbles are all very poor in K, while other marbles h common constituent of spinel-bearing assemblages, which can inclu The proportions of these minerals are expected to obey the followi Dol þ 2 Kþ ðaqÞ þ 4ð Þþ H2O; F CO2 $ 2 Phl þ 5 Cal ð1Þ 6 Fo þ Spl þ 2 Phl þ 7 Dol ð2Þ 6 Prg þ 3 Spl þ 9 Dol þ 12 Kþ ðaqÞþ12 Hð Þ 2O; F þ reactions, low K activity would favor spinel over phlogopite. The for calcite for the reaction to proceed, and thus K could be a limiting re incorporation of Al into phlogopite. Similarly, in some phlogopite-be rock, dolomite, pargasite, and spinel occur as a stable assemblage, l limiting factor in the phlogopite-forming reaction. The predominanc an Na-dominant fluid composition and reinforces the low-K hypoth and calcite-bearing diopsidite

$$3\,\mathrm{Di} + \mathrm{Spl} + 2\,\mathrm{Dol} + 2\,\mathrm{K^+}_{(aq)} + 4(\ldots$$
$$\leftrightarrow 2\,\mathrm{Phl} + 5\,\mathrm{Cal}$$

$$6\,\mathrm{Fo} + \mathrm{Spl} + 7\,\mathrm{Cal} + 2\,\mathrm{K^+}_{(aq)} + 4(\ldots$$
$$\leftrightarrow 2\,\mathrm{Phl} + 7\,\mathrm{Dol}$$

M.Belley et al, The Canadian Mineralogist Vol. 57, pp. 147-200 (2019)

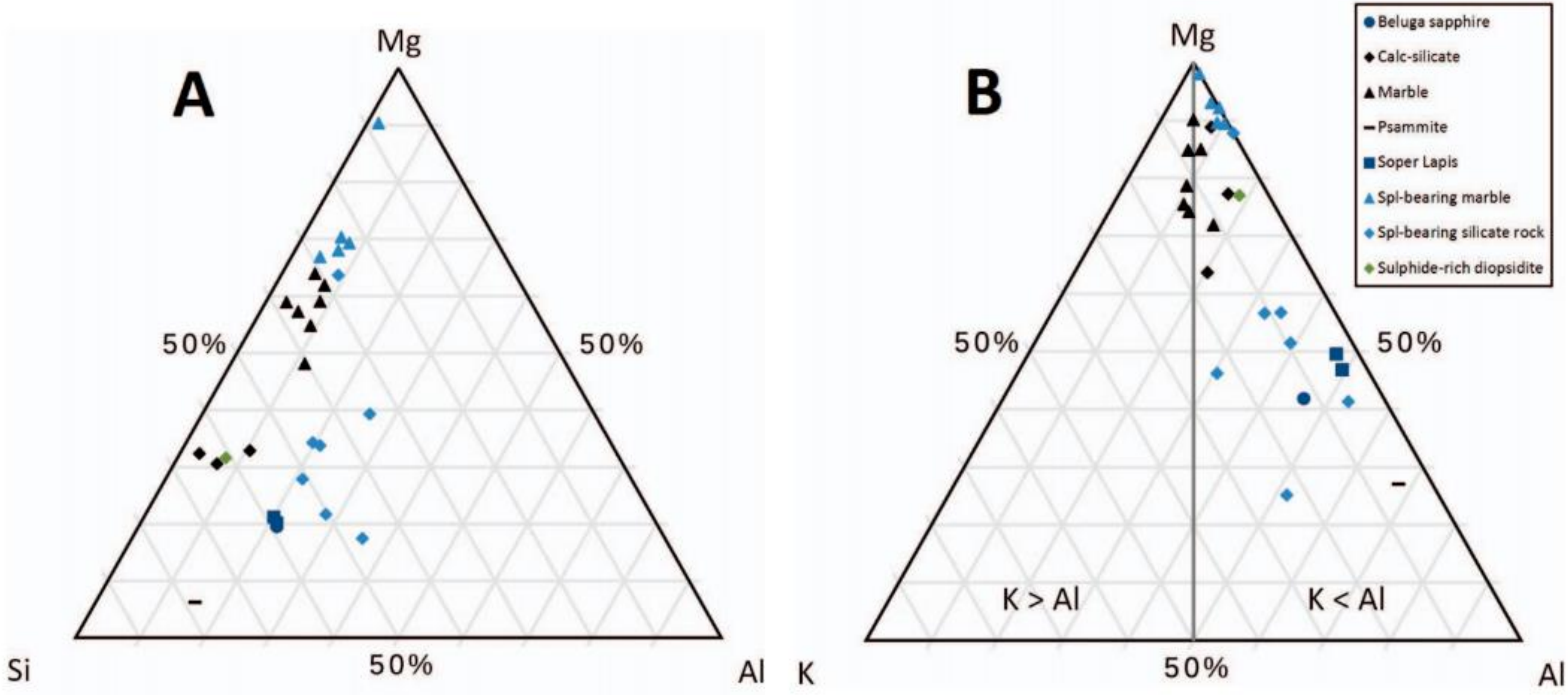

A
B
Mg
Si
Al
K
50%
K > Al
K < Al
Beluga sapphire
Calc-silicate
Marble
Psammite
Soper Lapis
Spl-bearing marble
Spl-bearing silicate rock
Sulphide-rich diopsidite

Field expedition

- Some of the gem producing areas visited

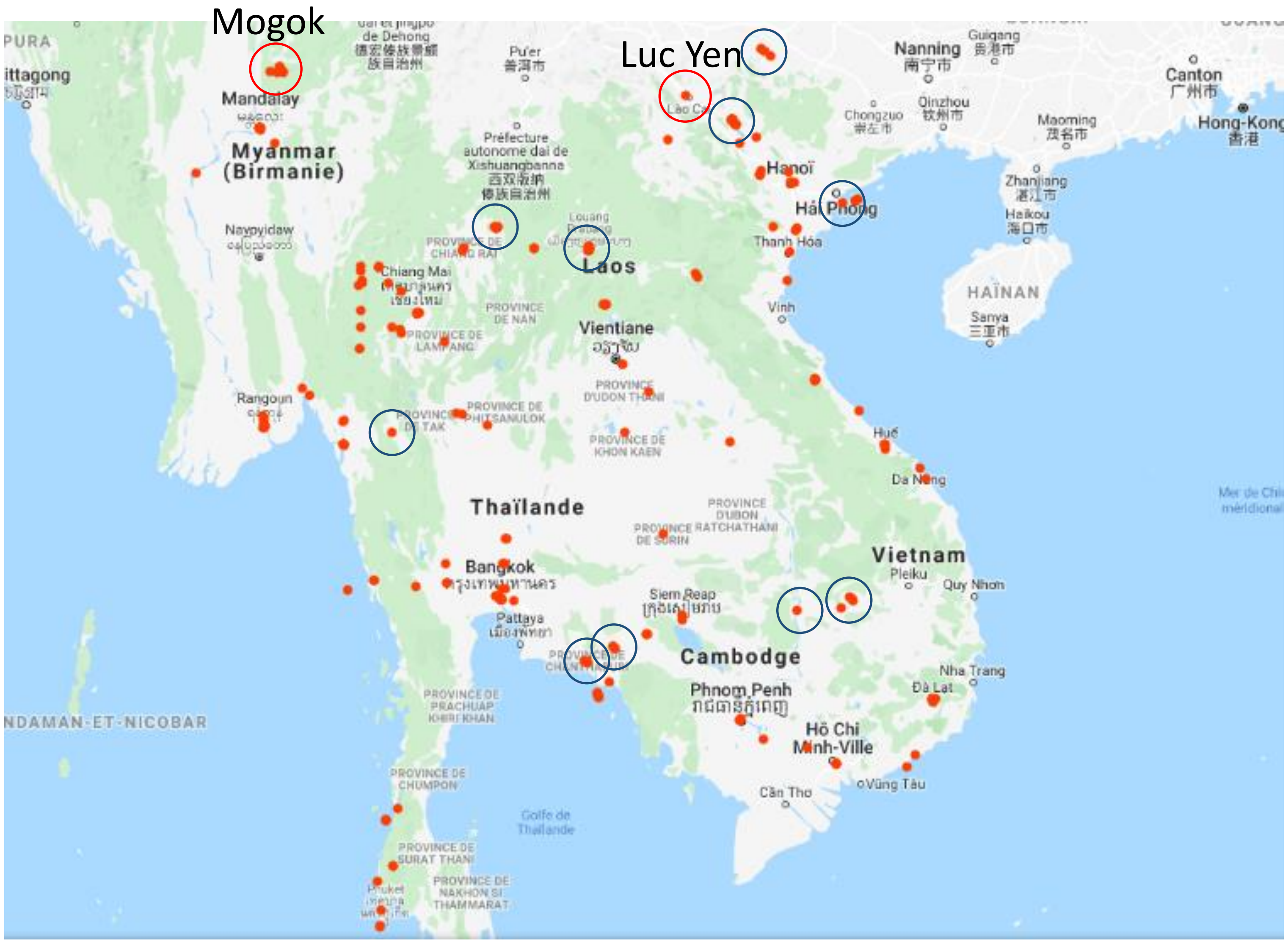

- (C, O)-isotopic analyses of carbonates from the marbles:
  - marbles acted as a metamorphic closed fluid system
  - weren’t infiltrated by externally-derived fluids.

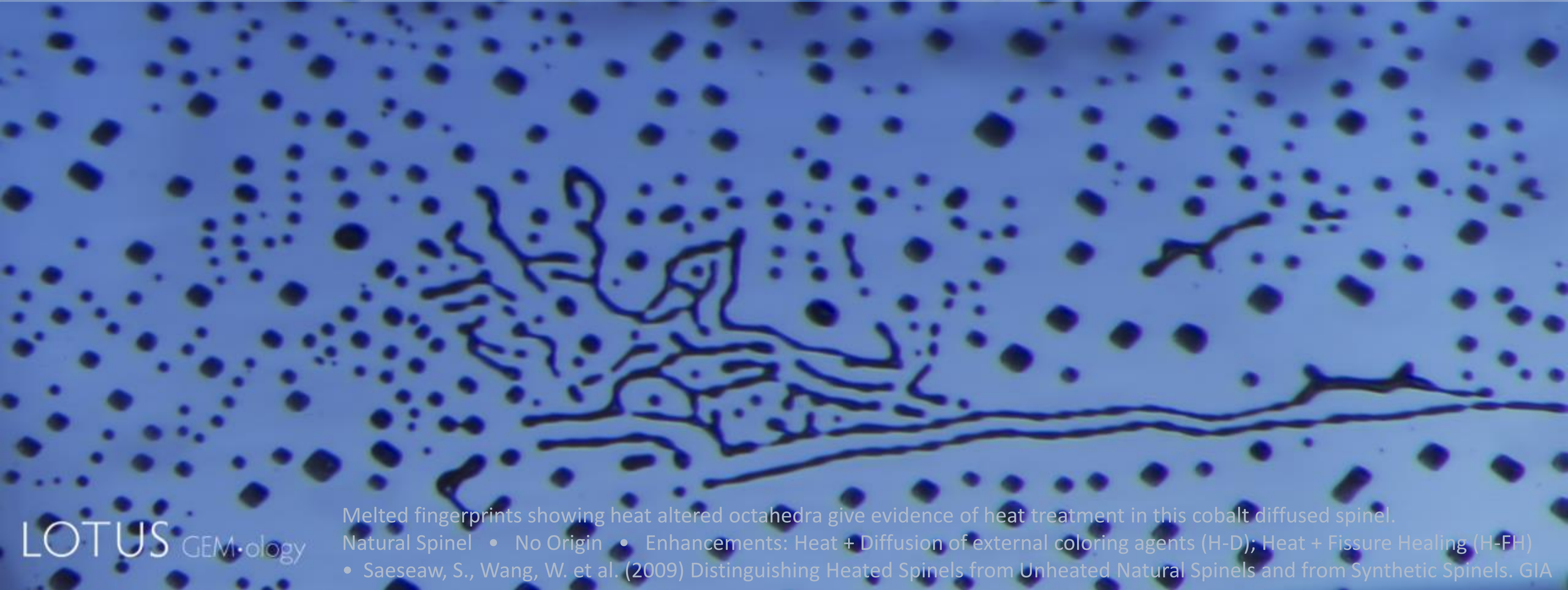

Melted fingerprints showing heat altered octahedra give evidence of heat treatment in this cobalt diffused spinel.
Natural Spinel • No Origin • Enhancements: Heat + Diffusion of external coloring agents (H-D); Heat + Fissure Healing (H-FH)
• Saeseaw, S., Wang, W. et al. (2009) Distinguishing Heated Spinels from Unheated Natural Spinels and from Synthetic Spinels. GIA

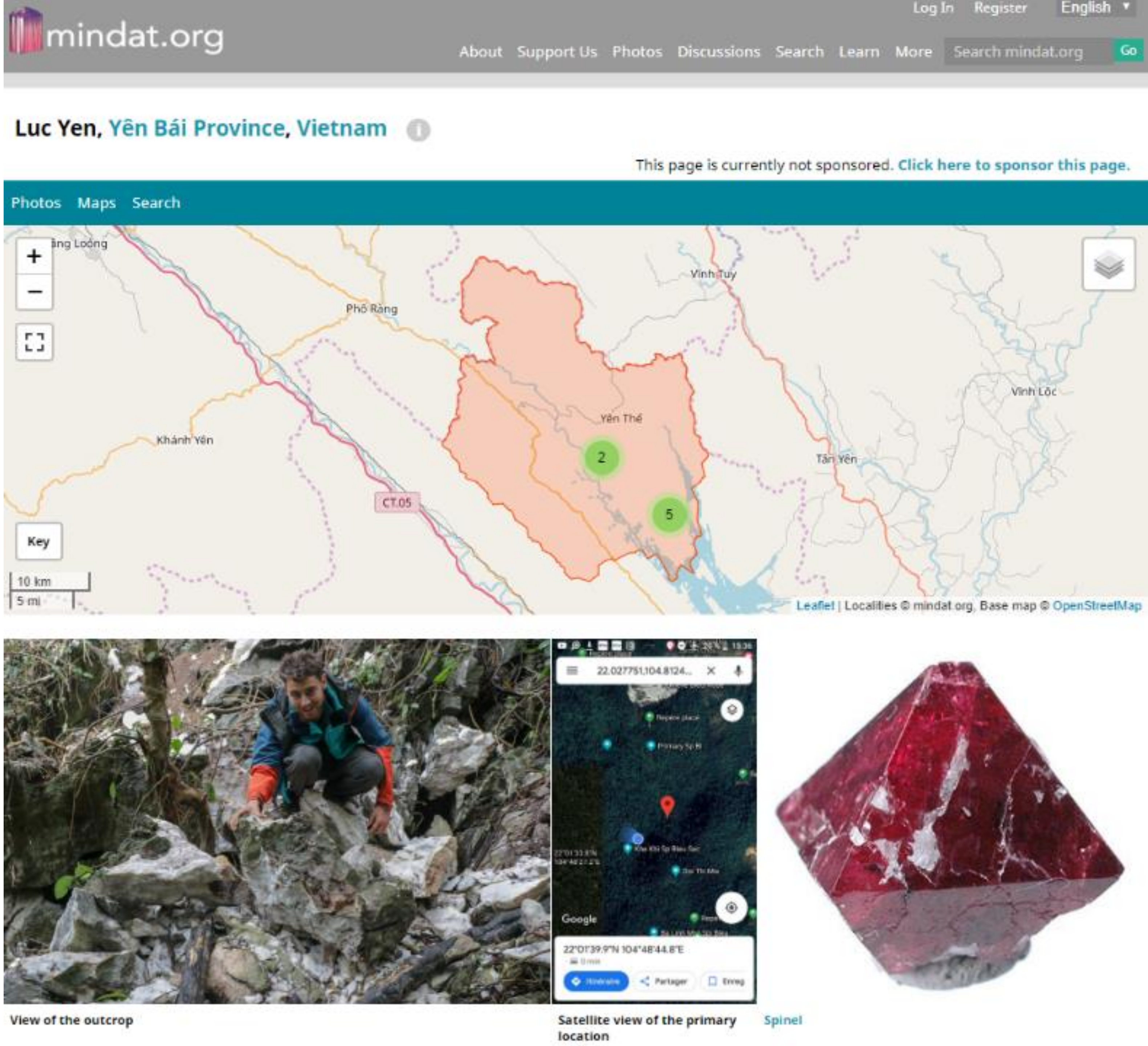
mindat.org
Log In
Register
English
About
Support Us
Photos
Discussions
Search
Learn
More
Search mindat.org
Go
Luc Yen, Yên Bái Province, Vietnam
This page is currently not sponsored. Click here to sponsor this page.
Photos
Maps
Search
Phô Ràng
Vinh Tuy
Yên Thế
Khánh Yên
Tân Yên
Vĩnh Lộc
CT.05
Key
10 km
5 mi
Leaflet | Localities © mindat.org, Base map © OpenStreetMap
View of the outcrop
Satellite view of the primary location
Spinel

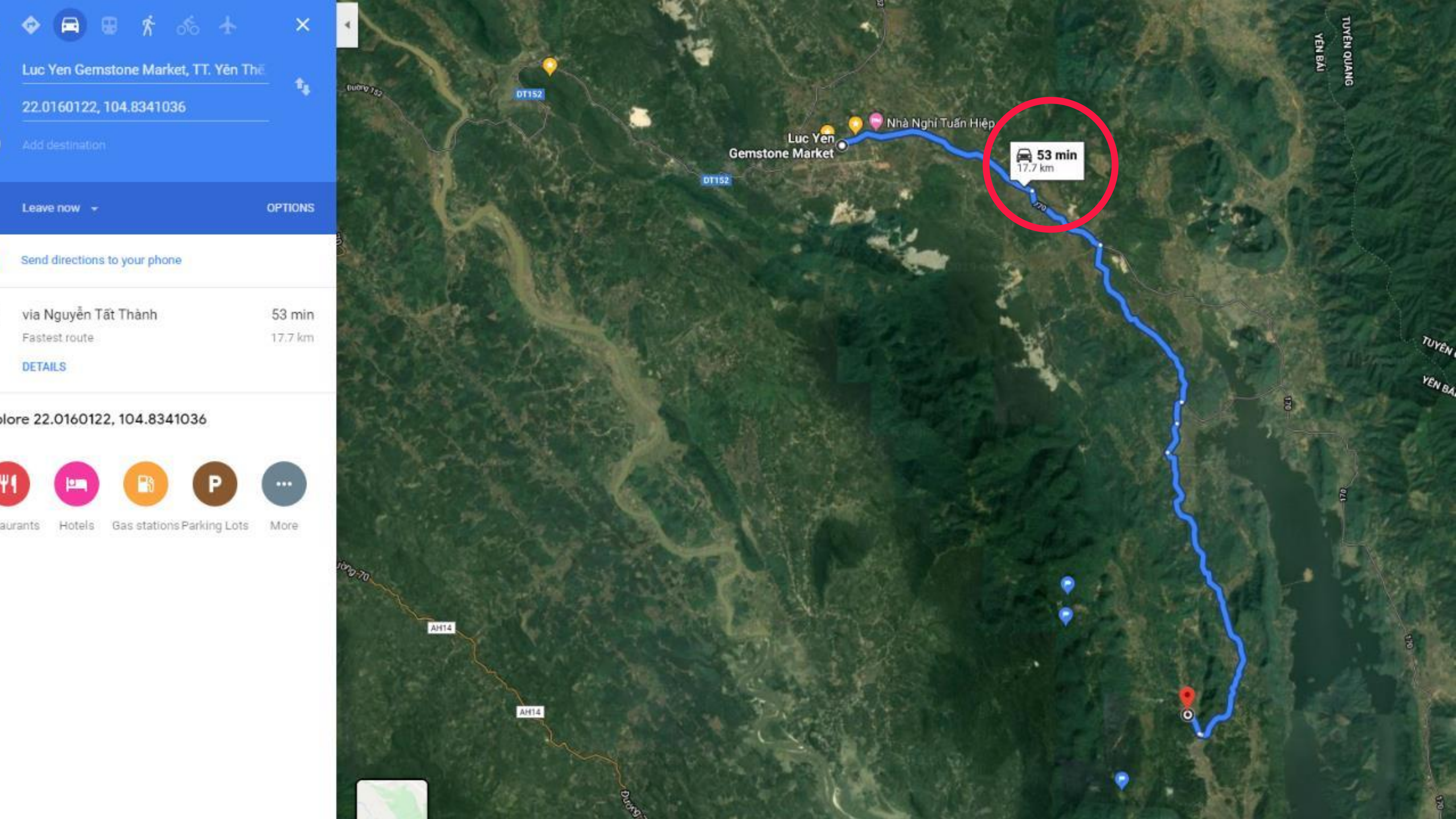
Luc Yen Gemstone Market, TT. Yên Thế
22.0160122, 104.8341036
Add destination
Leave now
OPTIONS
Send directions to your phone
via Nguyễn Tất Thành
53 min
Fastest route
17.7 km
DETAILS
plore 22.0160122, 104.8341036
aurants
Hotels
Gas stations
Parking Lots
More
Luc Yen
Gemstone Market
Nhà Nghỉ Tuấn Hiệp
53 min
17.7 km
DT152
DT152
AH14
AH14
YÊN BÁI
TUYÊN QUANG

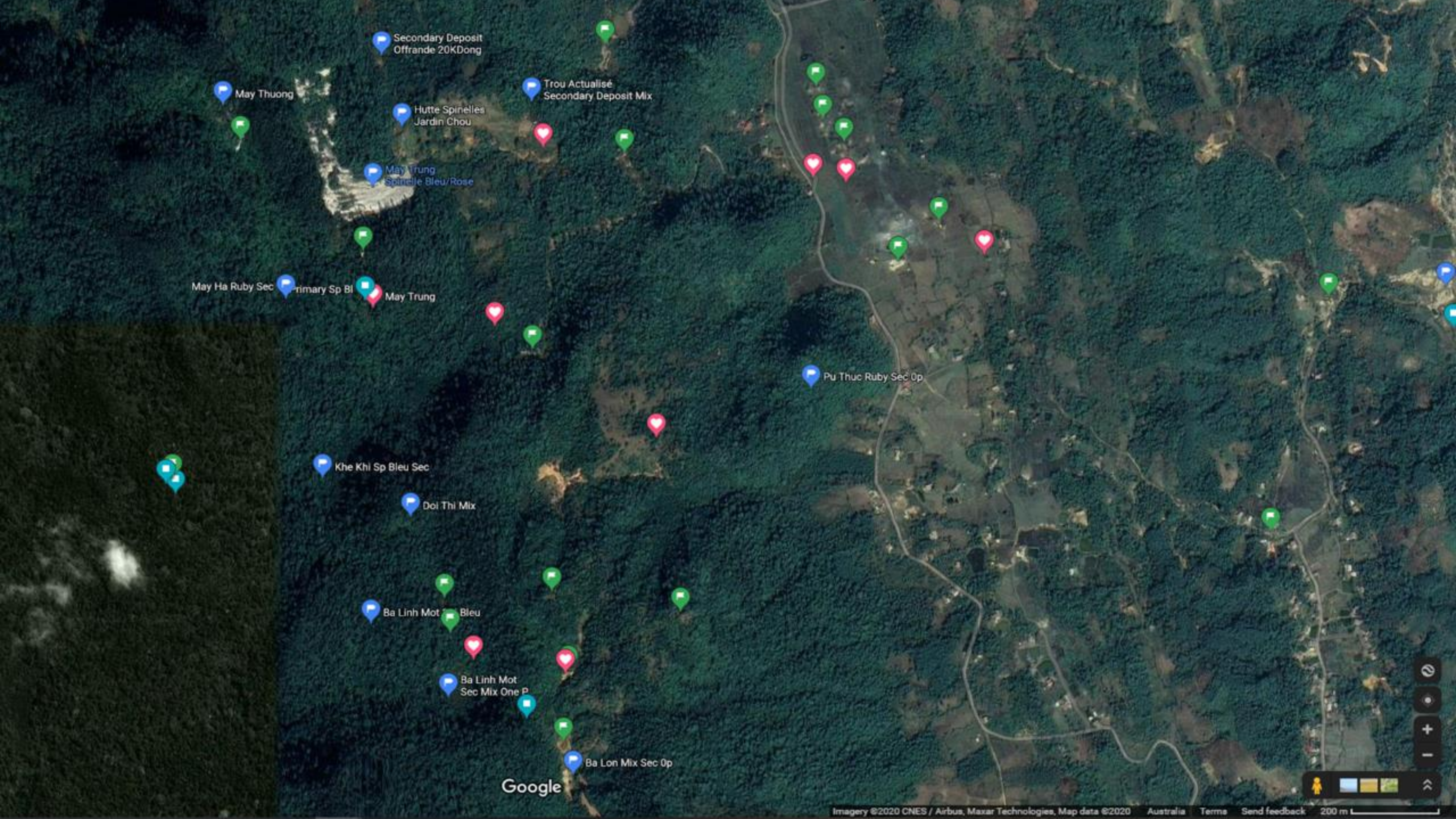
Secondary Deposit
Offrande 20KDong
May Thuong
Trou Actualisé
Secondary Deposit Mix
Hutte Spinelles
Jardin Chou
May Trung
Spinelle Bleu/Rose
May Ha Ruby Sec
rimary Sp Bl
May Trung
Pu Thuc Ruby Sec 0p
Khe Khi Sp Bleu Sec
Doi Thi Mix
Ba Linh Mot
Bleu
Ba Linh Mot
Sec Mix One P
Ba Lon Mix Sec 0p
Google
Imagery ©2020 CNES / Airbus, Maxar Technologies, Map data ©2020
Australia
Terms
Send feedback
200 m

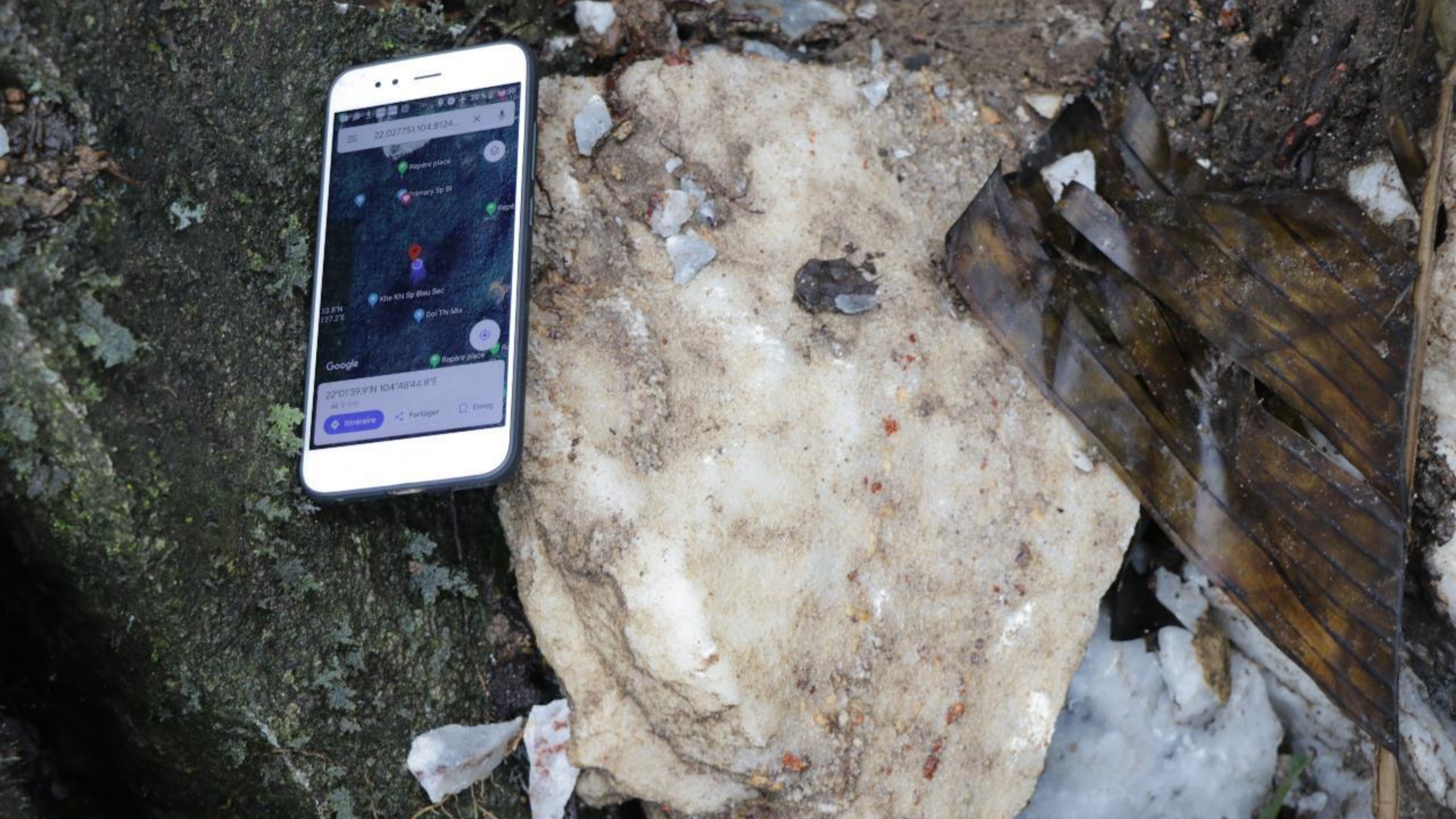
Repère place
Khe Khi Sp Bleu Sec
Google
Repère place
22°01'39.9"N 104°48'44.8"E
Partager






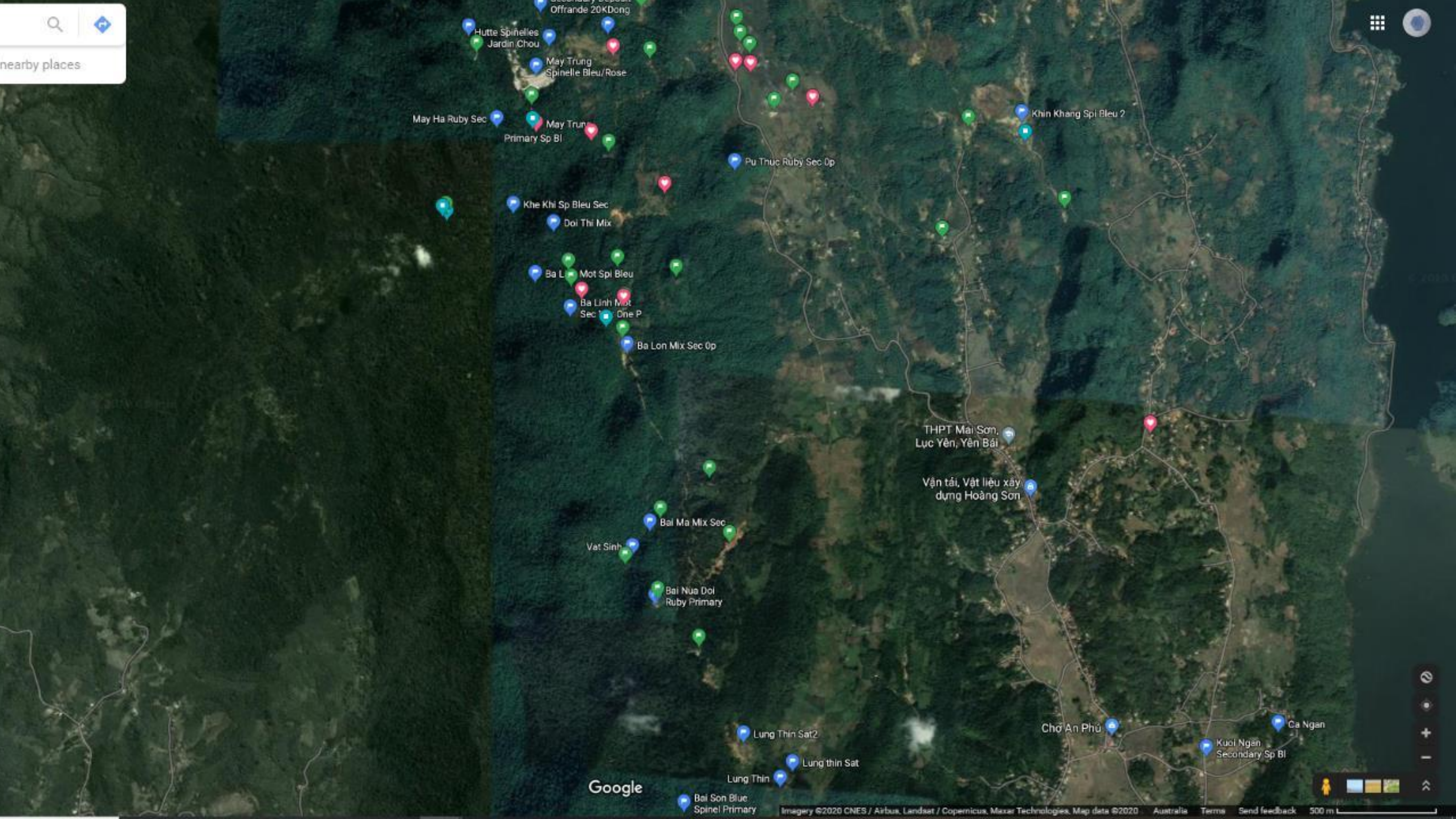
nearby places
Offrande 20KDong
Hutte Spinelles
Jardin Chou
May Trung
Spinelle Bleu/Rose
May Ha Ruby Sec
Primary Sp Bl
Pu Thuc Ruby Sec 0p
Khin Khang Spi Bleu 2
Khe Khi Sp Bleu Sec
Doi Thi Mix
Mot Spi Bleu
Ba Lon Mix Sec 0p
THPT Mai Sơn,
Lục Yên, Yên Bái
Vận tải, Vật liệu xây
dựng Hoàng Sơn
Bai Ma Mix Sec
Vat Sinh
Bai Nua Doi
Ruby Primary
Lung Thin Sat2
Lung thin Sat
Lung Thin
Bai Son Blue
Spinel Primary
Chợ An Phú
Ca Ngan
Kuoi Ngan
Secondary Sp Bl
Google
Imagery ©2020 CNES / Airbus, Landsat / Copernicus, Maxar Technologies, Map data ©2020 Australia Terms Send feedback 500 m

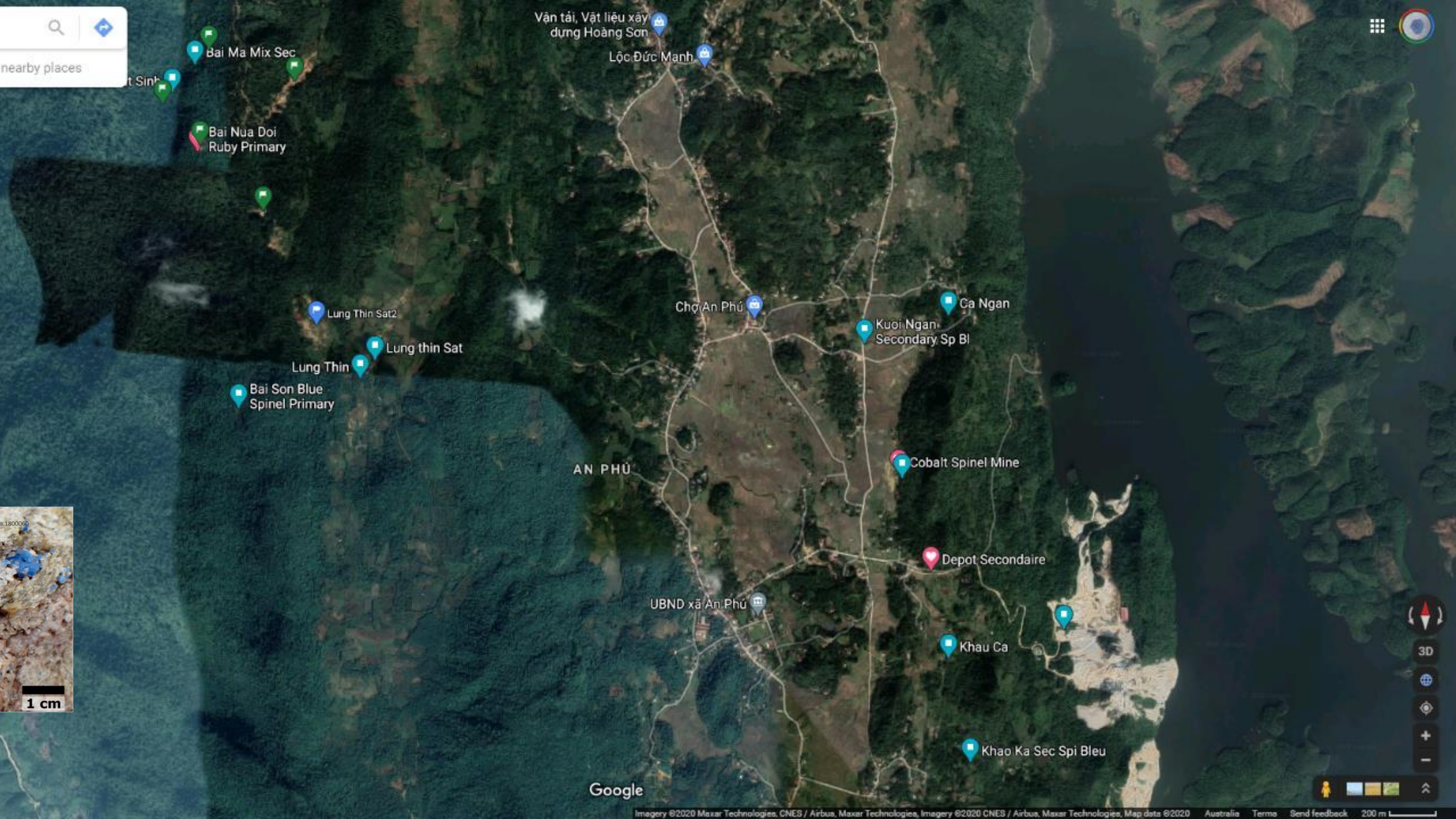
nearby places
Bai Ma Mix Sec
t Sinh
Bai Nua Doi
Ruby Primary
Vận tải, Vật liệu xây
dựng Hoàng Sơn
Lộc Đức Mạnh
Lung Thin Sat2
Lung thin Sat
Lung Thin
Bai Son Blue
Spinel Primary
Chợ An Phú
Ca Ngan
Kuoi Ngan
Secondary Sp Bl
AN PHÚ
Cobalt Spinel Mine
Depot Secondaire
UBND xã An Phú
Khau Ca
Khao Ka Sec Spi Bleu
1 cm
3D
Google
Imagery ©2020 Maxar Technologies, CNES / Airbus, Maxar Technologies, Imagery ©2020 CNES / Airbus, Maxar Technologies, Map data ©2020
Australia
Terms
Send feedback
200 m

Are there Aussie blue spinels ?

- Yes ! Murchison carbonaceous chondrite.
- Only occurrence I could find
- Likely a deceptive greyish “blue”…

Consider the analyses of terrestrial kaersutite (Table 1). The $^{25}Mg/^{24}Mg$ ratio varied by about 4 permil over the two week time period covering the analyses. This variation is due to variable instrumental parameters, such as the secondary-ion transfer optics, but has not been systematically investigated. However, variation over a daily period is much smaller. In order to monitor the instrumental mass fractionation, terrestrial kaersutite analyses were taken interspersed with the analyses of the different Murchison mineral phases. For this purpose a 7 mm hole was cast in the standard one inch epoxy discs to mount a plug containing the terrestrial kaersutite in the same ion-optical plane. Generally, an analysis of the kaersutite was made at least at the beginning and end of a day's analyses.

The observed instrumental fractionation is also matrix dependent, that is, the measured magnesium isotopic composition depends on the mineral phase analysed. The matrix dependence was monitored on three separate occasions (Table 1). Four of the phases, kaersutite, hibonite, olivine, and pyroxene, show similar isotopic fractionation but spinel is some 6 permil lower. Matrix-correction factors were determined from these terrestrial sample analyses so that a correction could be applied when using the terrestrial kaersutite as a standard for the Murchison mineral analyses. The fractionation factor, F_{mat}, is the ratio of the $^{25}Mg/^{24}Mg$ measured for a given terrestrial mineral species relative to the $^{25}Mg/^{24}Mg$ for terrestrial kaersutite, *i.e.*

$$F_{mat} = \frac{(^{25}Mg/^{24}Mg)_{min}}{(^{25}Mg/^{24}Mg)_{kar}}.$$

These measurements were taken with a time period of a few hours to minimise effects of the variable instrumental fractionation. The matrix-correction factors have no effect on the residual $\delta^{26}Mg$.

The intrinsic fractionation of the sample can then be derived by correcting for the variable instrumental fractionation and for matrix-dependent fractionation. The intrinsic magnesium isotopic fractionation, $\Delta^{25}Mg$ (in permil), is expressed in delta notation relative to terrestrial as

$$\Delta^{25}Mg = \left[\frac{(^{25}Mg/^{24}Mg)_{meas}}{(^{25}Mg/^{24}Mg)_{kar} \cdot F_{mat}} - 1\right] \times 1000$$

where $(^{25}Mg/^{24}Mg)_{meas}$ is the measured raw $^{25}Mg/^{24}Mg$ ratio for the phase under analysis, $(^{25}Mg/^{24}Mg)_{kar}$ is the raw $^{25}Mg/^{24}Mg$ ratio for the terrestrial kaersutite, and F_{mat} is the matrix-correction factor for the phase relative to the kaersutite.

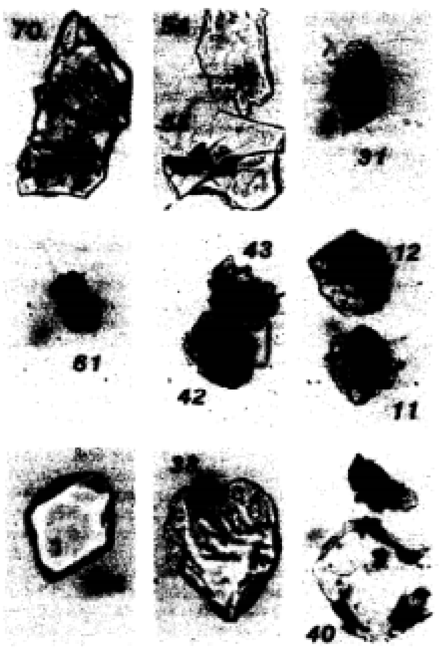

FIG. 2. Representative photomicrographs of Murchison phases analysed in this study. Hibonite grains #54, #55, and #70 are colourless crystal plates in contrast to grains #31, #43, #61 which are deep-blue in colour and granular. This distinction is also noted in grain chemistry (Table 3), with the platey hibonites having low substitution of MgO and TiO_2 and the granular hibonites having high substitution of these elements. Spinels range from microcrystalline (grains #42, #12), to optically uniform (grain #11), to euhedral crystals (grain #68). Inclusions of hibonite and perovskite are common (grain #11). Olivines range from microcrystalline (grain #40) to optically uniform (grain #38) and are anhedral. Inclusions of iron sulphides and oxides are common. (Transmitted light, long dimension of photographs ≈100 μm.)

SAMPLE DESCRIPTION

The grains analysed in this study were extracted from 67 g of small Murchison fragments which were crushed to pass a 400 μm mesh, with further sieving to collect the 40–75 μm fraction. The denser fraction ($\rho > 3.3$ g/cm^3) was separated in methylene iodide and the non-magnetic fraction was collected after magnetic separation in an alcohol suspension. The resulting concentrate was handpicked for blue grains in a search for hibonite (IRELAND *et al.*, 1985), but contained a large proportion of spinel and some olivine. The grains were mounted in epoxy and polished in preparation for analysis.

The hibonite grains analysed were predominantly mono-mineralic with only one grain (#31) containing a 5 μm perovskite inclusion. Three of the grains (#31, #43, #61) are deep blue granular aggregates of <5 μm hibonite laths and granules, whereas the other five (#20, #52, #54, #55, #70) are essentially colourless single crystal plates (Fig. 2). This distinction is also recognised in the electron probe chemical analyses with the deep blue grains having markedly higher MgO and TiO_2 contents than the colourless hibonites (Table 3).

The blue spinels are essentially stoicheiometric $MgAl_2O_4$ with minimal (<1% total) substitution of Cr, V, and Fe. The spinels range from anhedral microcrystalline grains, to anhedral optically uniform grains, to euhedral crystals (Fig. 2). Small (<5 μm) inclusions of hibonite and perovskite are common.

The olivine grains were essentially a contaminant from the handpicking process. They are light green and texturally range from microcrystalline to optically uniform anhedral grains (Fig. 2). Iron oxide and sulphide inclusions are common. Four of the grains have Mg numbers [100 × Mg/(Mg + Fe)] greater than 98, while grain #38 has an Mg number of 50.

Applications :

ACS Catalysis

pubs.acs.org/acscatalysis Letter

Cobalt Aluminate Spinel as a Cocatalyst for Photocatalytic Oxidation of Water: Significant Hole-Trapping Effect

Tomoki Kanazawa, Kosaku Kato, Ryusei Yamaguchi, Tomoki Uchiyama, Daling Lu, Shunsuke Nozawa, Akira Yamakata,* Yoshiharu Uchimoto, and Kazuhiko Maeda*

Cite This: *ACS Catal.* 2020, 10, 4960–4966 Read Online

ACCESS | Metrics & More | Article Recommendations | Supporting Information

ABSTRACT: Here we show that nanoparticulate $CoAl_2O_4$ spinel serves as an efficient cocatalyst for photocatalytic oxidation of water. The O_2 evolution activity of $CoAl_2O_4$/g-C_3N_4 from an aqueous solution of $AgNO_3$ under visible light irradiation was ~10 times that of unmodified g-C_3N_4 and also exceeded that of an analogue modified with a well-known Co_3O_4 cocatalyst for each optimal preparation condition. Transient absorption spectroscopy indicated that the $CoAl_2O_4$ cocatalyst with Co^{2+} as the main cobalt species at the A site of the spinel possessed better hole-capturing properties than the Co_3O_4 cocatalyst, which was the main reason for the improved water-oxidation performance.

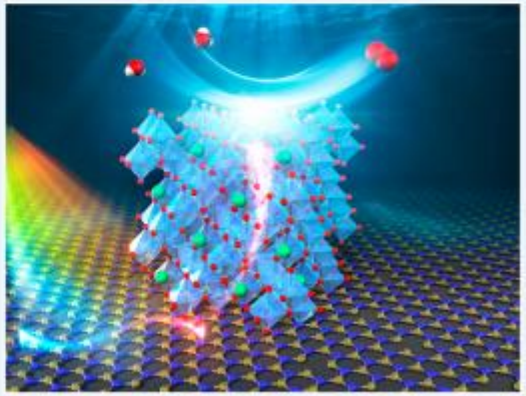

KEYWORDS: *artificial photosynthesis, mixed anion compounds, solar fuels, visible light, water splitting*

Applications :

Abbasi Asl, E., Haghighi, M., & Talati, A. (2020). *Enhanced Simulated Sunlight-Driven Magnetic MgAl2O4-AC Nanophotocatalyst for Efficient Degradation of Organic Dyes. Separation and Purification Technology, 117003.* doi:10.1016/j.seppur.2020.117003

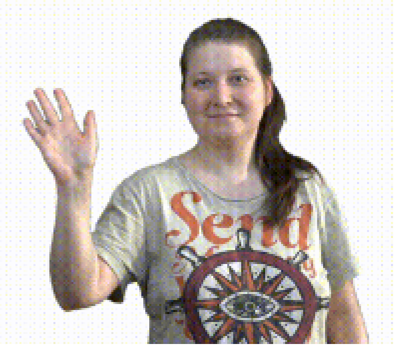

Enhanced Simulated Sunlight-Driven Magnetic $MgAl_2O_4$-AC Nanophotocatalyst for Efficient Degradation of Organic Dyes

Ebrahim Abbasi Asl[1,2], Mohammad Haghighi[*,1,2], Azadeh Talati[1,2]

1. *Chemical Engineering Faculty, Sahand University of Technology, P.O.Box 51335-1996, Sahand New Town, Tabriz, Iran.*

2. *Reactor and Catalysis Research Center (RCRC), Sahand University of Technology, P.O.Box 51335-1996, Sahand New Town, Tabriz, Iran.*

Applications :

sci-hub

to open science

⇣ save

Diaz-Torres, L. A., Mtz-Enriquez, A. I., Garcia, C. R., Coutino-Gonzalez, E., Oliva, A. I., Vallejo, M. A., … Oliva, J. (2020). *Efficient hydrogen generation by ZnAl2O4 nanoparticles embedded on a flexible graphene composite. Renewable Energy.* doi:10.1016/j.renene.2020.01.074

url to share this paper:
sci-hub.se/10.1016/j.renene.2020.01.074

versions:
from 2020-01-30
from 2020-07-11

Sci-Hub is a project
to make knowledge free
support →

Renewable Energy 152 (2020) 634–643

Contents lists available at ScienceDirect

Renewable Energy

journal homepage: www.elsevier.com/locate/renene

ELSEVIER

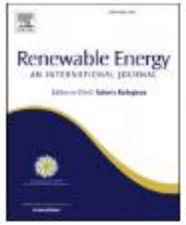

Efficient hydrogen generation by $ZnAl_2O_4$ nanoparticles embedded on a flexible graphene composite

L.A. Diaz-Torres [a], A.I. Mtz-Enriquez [b], C.R. Garcia [c], E. Coutino-Gonzalez [d], A.I. Oliva [e], M.A. Vallejo [f], T. Cordova [f], C. Gomez-Solis [f, **], J. Oliva [g, *]

[a] Grupo de Espectroscopia de Materiales Avanzados y Nanoestructurados, GEMANA, Centro de Investigaciones en Óptica A.C., 37150, Leon, Guanajuato, Mexico
[b] Cinvestav IPN, Unidad Saltillo, Parque Industrial, Ramos Arizpe, Coahuila, 25900, Mexico
[c] Facultad de Ciencias Físico-Matemáticas, Universidad Autónoma de Coahuila, 25000, Saltillo Coahuila, Mexico
[d] CONACYT - Centro de Investigaciones en Óptica, A. C. Loma del Bosque 115, Colonia Lomas del Campestre, León, Guanajuato, 37150, Mexico
[e] Cinvestav IPN, Unidad Mérida, Depto. de Física Aplicada, Mérida, Yucatán, 97310, Mexico
[f] Departmento de Ingeniería Física, Universidad de Guanajuato, 37150, Leon, Mexico
[g] CONACYT- División de Materiales Avanzados, Instituto Potosino de Investigación Científica y Tecnológica A. C., 78216, San Luis Potosí SLP, Mexico

ARTICLE INFO

Article history:
Received 11 April 2019
Received in revised form
28 December 2019
Accepted 17 January 2020
Available online 22 January 2020

ABSTRACT

This work reports the hydrogen generation properties of $ZnAl_2O_4$ (ZAO) powders synthesized by a combustion method, which produced carbon dots (C-dots) on the ZAO surface. These ZAO nanoparticles decorated with C-dots were incorporated into a polyacrylate matrix to form a photocatalytic membrane (named PAZO), which was subsequently attached to a flexible graphene composite (FGC) to form a FGC/PAZO (GAZO) composite. The morphological analysis by scanning electron microscopy shows embedded ZAO nanoparticles with sizes of 20–90 nm into the polymeric matrix. In addition, hydrogen generation

Applications :

JOURNAL OF RAMAN SPECTROSCOPY
J. Raman Spectrosc. 2004; **35**: 646–649
Published online in Wiley InterScience (www.interscience.wiley.com). DOI: 10.1002/jrs.1210

JRS

Raman investigation of ceramics from 16th and 17th century Portuguese shipwrecks

Danita de Waal*

Department of Chemistry, University of Pretoria, 0002 Pretoria, South Africa

Received 5 September 2003; Accepted 8 March 2004

Raman spectra were recorded of the various components of a series of about 20 ceramic shards from nine Portuguese ships that were wrecked around the South African coast between 1550 and 1650. α-Quartz was a typical component of the porcelain body. The blue pigment could be identified as $CoAl_2O_4$, or cobalt blue, and the glaze covering the ceramic surface presented a series of broad Raman bands typical of amorphous silicates. One shard from the Santa Maria Madre de Deus, which looked different form the other shards, was shown not to be a porcelain owing to the various components ($CaCO_3$, $CaSO_4 \cdot 2H_2O$ or gypsum, amorphous carbon, anatase) which could be identified in the ceramic. This is an indication that this one piece is unlikely to be of the same Chinese origin as the Ming porcelain shards.

To recap:

Spinel 101 : chemical formula

Trace elements and color

What is a cobalt spinel ?

Condition of formation

Petrological assemblage

Occurrences